LA-3607-MS

C.3

LOS ALAMOS SCIENTIFIC LABORATORY
of the
University of California
LOS ALAMOS • NEW MEXICO

Quarterly Status Report on the Advanced Plutonium Fuels Program for Period July 1 - September 30, 1966

(First Report)

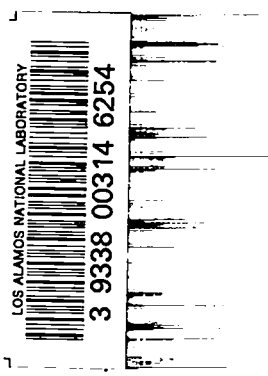

UNITED STATES
ATOMIC ENERGY COMMISSION
CONTRACT W-7405-ENG. 36

All LA...MS reports are informal documents, usually prepared for a special purpose. This LA...MS report has been prepared, as the title indicates, to present the status on the LASL Advanced Plutonium Fuels Program. It has not been reviewed or verified for accuracy in the interest of prompt distribution. All LA...MS reports express the views of the authors as of the time they were written and do not necessarily reflect the opinions of the Los Alamos Scientific Laboratory or the final opinion of the authors on the subject.

LA-3607-MS
Special Distribution

LOS ALAMOS SCIENTIFIC LABORATORY
of the
University of California
LOS ALAMOS • NEW MEXICO

Report compiled: October 1966
Report distributed: October 31, 1966

Quarterly Status Report on the Advanced Plutonium Fuels Program for Period July 1 - September 30, 1966

(First Report)

FOREWORD

This report is the first in a series which will describe work on the Advanced Plutonium Fuels Program at the Los Alamos Scientific Laboratory. The program is more general than its title might imply. Studies related to the possible use of mixed plutonium and uranium carbides as fast breeder reactor fuels form a major portion of the planned tasks, but in addition, the program includes investigations categorized as "sodium coolant technology development." Some effort is also devoted to general problems in fast reactor physics, as well as to the development of certain types of instrumentation, or of technology which should be of interest to the AEC's LMFBR program. Specific areas of investigation are identified by the reference to appropriate Form 189a number.

These progress reports, which are to be issued on a quarterly basis, will present status of the work, plans for the next stages of the task, and, as they become available, the data obtained. Generally, these data will indicate preliminary results. In the fourth quarter, an annual report, the year's result will be summarized, and where possible, final, quantitative data will be presented.

PROJECT 801

DISTRIBUTION AND DECONTAMINATION OF FISSION PRODUCTS IN CONTAMINATED SODIUM SYSTEMS

Person in Charge: D. B. Hall

Principal Investigators: R. H. Perkins
J. C. Clifford

I. INTRODUCTION

The behavior of fission products released to sodium coolant from tramp uranium or from failed or deliberately vented reactor fuel elements may limit access to the primary coolant system and affect the consequences of a loss-of-coolant incident. Depending on the fission product inventory anticipated in the primary coolant, it may be desirable to concentrate uranium, plutonium, long-lived energetic gamma-emitting isotopes, and shorter lived biologically hazardous isotopes at specific locations within the primary system.

To this end we are investigating the interaction of plutonium-based fuels with sodium, the release and distribution of fission products from irradiated fuel to sodium, and methods by which this distribution may be altered. The techniques and preliminary results from a study of the distribution and trapping of long-lived fission products in sodium systems are described below.

In these experiments irradiated fuel and sodium are contacted in a small forced convection sodium loop. *In situ* gamma-ray spectrometry is the principal analytical tool, augmented by wet radiochemical analyses. These loop experiments are used to determine the general distribution of fission products in a sodium system and the relative effectiveness of trapping techniques on this distribution. Trapping techniques that show some merit will be examined in more detail in capsule experiments.

II. FORCED CONVECTION SODIUM LOOP

(J. C. Clifford)

A. Experimental Apparatus and Techniques

A schematic representation of the forced convection sodium system used to study transport and trapping of fission products is shown in Fig. 1. The loop consists of three vertical legs, an electrical heater, an air vent dump, and a regenerative heat exchanger. The loop is constructed from types AISI 316 and 321 stainless steels and contains approximately 83 $in.^3$ of sodium. One leg is lead-shielded, and accepts irradiated fuel in an open-mouth tantalum container. The container and fuel are inserted and removed through a gas lock and a shielded handling can at the top of the column. The other vertical legs accept specimens of various materials held in 5 in.-long by 1-in.-diameter baskets. These materials are inserted and removed in the same manner as the fuel. A section of piping in one vertical specimen leg is removable, allowing insertion of traps into the system.

The loop can be operated isothermally at temperatures below 600°C or, as an extreme, the fuel leg and one specimen leg can be maintained at 600°C with the other specimen leg at 150°C. (The fuel leg and the adjacent specimen leg operate at the same temperature.) The maximum sodium flow is 300 lb/h.

The vertical leg containing the air cooler (the low temperature specimen leg) can be scanned to locate gamma-emitters, using a lead-collimated 3 in. x 3 in. NaI (Tl) scintillation detector housed in a 16-in.-diam, 24-in.-long lead shield. The photomultiplier output from the detector is fed to a 400 channel pulse height analyzer. The detector assembly can be moved approximately 3 ft in the vertical direction and can be positioned with an accuracy better than 0.005 in.

B. Summary of Experimental Results

Although no impurity determinations were made on sodium from this loop, experience with other zirconium hot-trapped loops of the same size

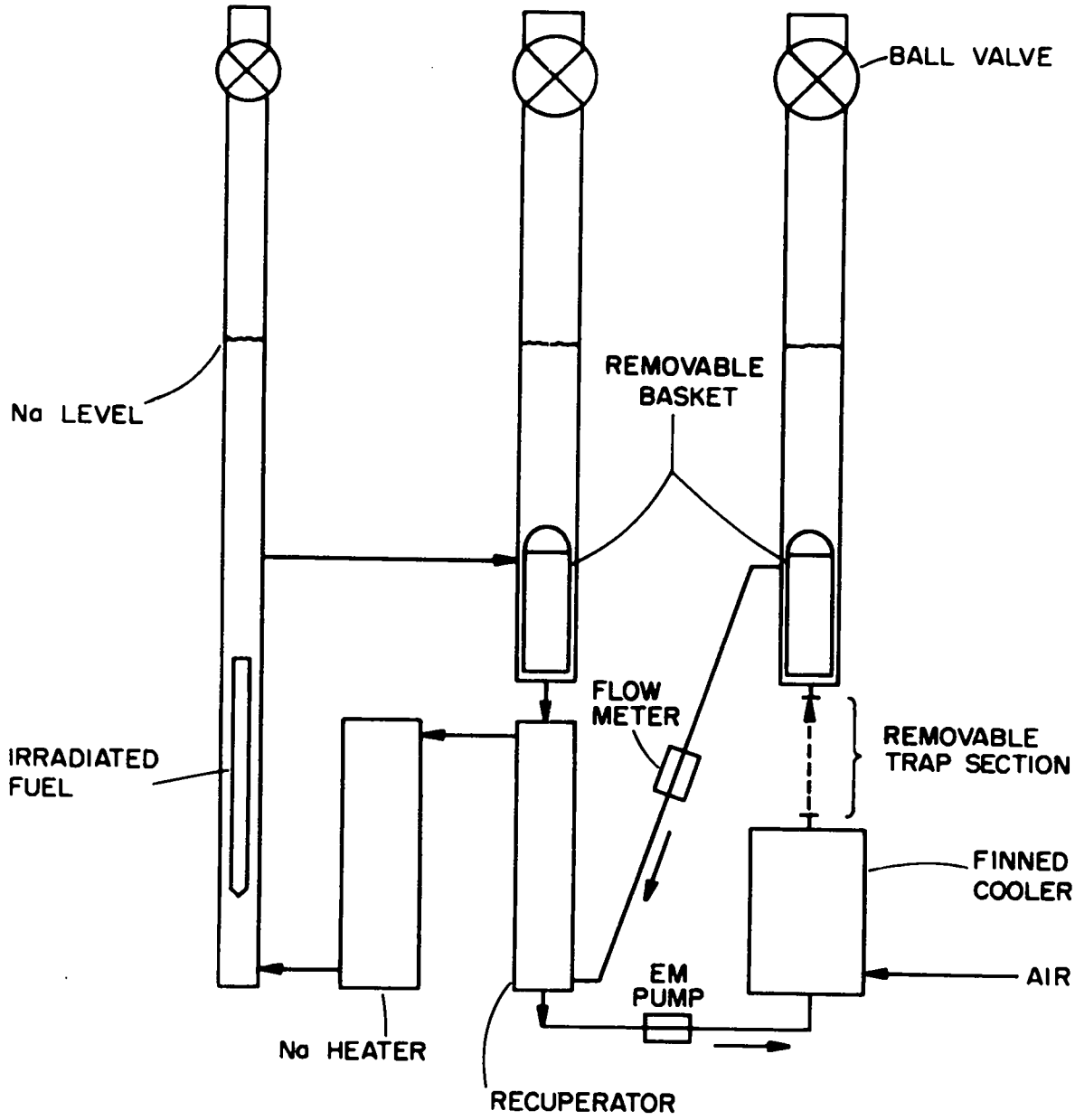

Fig. 1. Schematic Representation of Sodium Forced Convection Loop

and construction suggests that the oxygen content was maintained below 5 ppm. Typical values for carbon, hydrogen and nitrogen are ≤15, ≤10, and ≤3 ppm, respectively. The first fission product source, contained in an open-mouth, 7/16-in.-diam tantalum capsule, was immersed in the sodium at a temperature of 600°C. This source consisted of 5 g of a Pu-Co-Ce alloy containing 34 w/o plutonium, irradiated to a level of 2.5×10^{18} fissions and cooled for 2-1/2 years.

From a consideration of the chemical species involved, and from previous measurements of the distribution of fission products between irradiated, liquid Pu-Co-Ce alloy and sodium, it was anticipated that at least 0.9 of each of the long lived fission products ^{137}Cs, ^{90}Sr, and ^{155}Eu extracted to the sodium phases. Of these, ^{137}Cs was identified in the low temperature specimen leg a few hours after the fuel had been immersed. Because of the low energy of its principle gamma ray (0.087 MeV), ^{155}Eu was not detected by *in situ* gamma-ray spectrometry, although it was found in substantial quantity on materials later removed from the system. The strontium isotope, a beta-emitter, was detected only by removing materials from the loop.

Within 48 h after fuel addition, the ^{137}Cs activity in the 500°C low temperature specimen leg had reached a maximum. The majority of this activity was distributed, nonuniformly, within a 5-in. section of tubing packed with stainless steel wire mesh. The section is identified in Fig. 1 as the "removable trap section." During the next 800 h the amount of ^{137}Cs in the mesh decreased 20%, with 17% of this decrease occurring in the first 200 h. The remainder of the low temperature specimen leg exhibited no significant change in activity distribution or level.

Attempts were made to influence the distribution of ^{137}Cs by decreasing the temperature in the low temperature specimen leg while maintaining the remainder of the system at 600°C. Activity increases of 3 to 5% occurred shortly after each 70°C temperature drop. These were limited to the mesh section and, over a several hundred hour period at the new temperature, were offset by a gradual decline in activity.

After the low temperature leg had been cooled to 300°C without significant effect, the leg was raised back to 500°C, also without significant effect. Next, a longer temperature perturbation was impressed by cooling the low temperature leg to 300°C for 650 h. By the end of the period, the stainless steel mesh section had lost half of its ^{137}Cs activity. The rate of loss was constant during the period. The zirconium hot traps then were removed from the loop and sodium samples were withdrawn.

The fate of cesium activity leaving the stainless steel mesh (and, to a lesser extent, the loop piping) during this period is illustrated in Fig. 2. Here, the distribution of ^{137}Cs within the low temperature leg is shown 3200 h after the irradiated fuel was contacted with hot trapped sodium. This distribution does not represent an equilibrium condition, but illustrates the direction in which ^{137}Cs is moving. The larger ^{137}Cs deposit appears in the helium-filled gas space, in a 3-in. ring coinciding with the top of the thermal insulation. The second ^{137}Cs deposit extends through the 5-in. wire mesh section and its point of maximum activity is the leading, or upstream, edge of the section. The integrated activities in the deposits are in the ratio 2.3:1. Cesium was detected in the finned cooler, in the zirconium hot trap and in the connecting tubing, but at a level negligible compared with that in the mesh. The remaining sodium-filled portion of the system showed the same "background" gamma activity levels as had been found in the low temperature leg. The gas spaces in the high temperature and low temperature specimen legs contained approximately equal quantities of cesium, while the fuel leg gas space contained 15% as much.

To provide a quantitative estimate of the ^{137}Cs inventory in various portions of the system, integrated counting rates for gas space, stainless mesh, and bare tubing were corrected for geometric attenuation, scattering, detection efficiency and mass absorption. The results, after 3200 h of operation, are shown in Table I along with the original ^{137}Cs inventory in the fuel. The agreement between the system activity balance and the amount of cesium available from the fuel is fortuitous in view of the

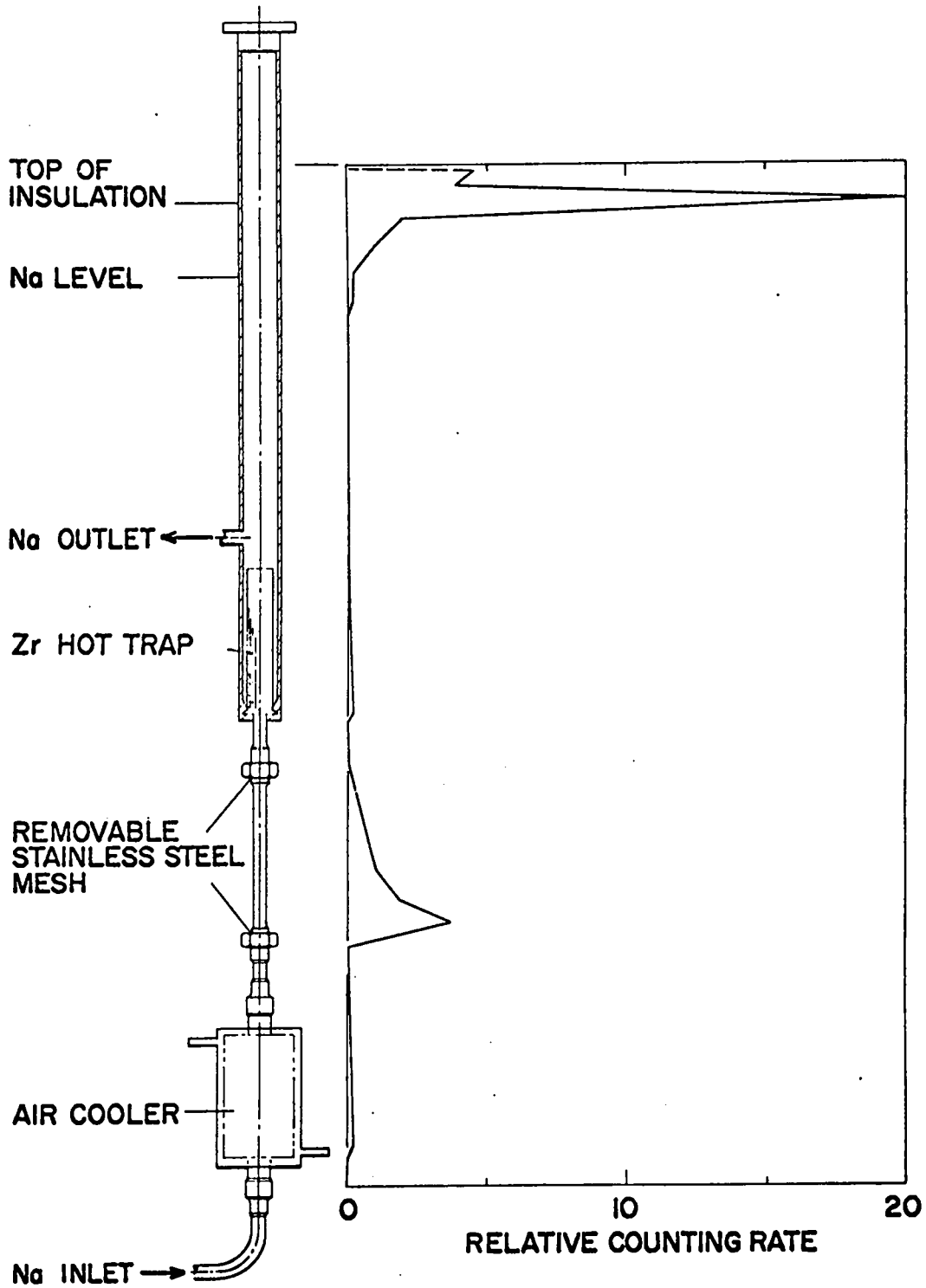

Fig. 2. Distribution of ^{137}Cs in Low Temperature Leg After 3200 h

TABLE I

Distribution of ^{137}Cs in a Hot Trapped Sodium After 3200 Hours of Operation

Location	Activity (d/m β)	% of Total	Average Activity Per Unit Surface (d/m/in.^{2})
Gas phase	3.58×10^9	57	3.8×10^8
Stainless steel mesh	0.77×10^9	12	7.7×10^7
Hot traps and stainless steel tubing	1.93×10^9	31	4.7×10^6
Total	6.28×10^9		
^{137}Cs inventory in original fuel	6.37×10^9		

assumptions involved in making the balance. Nevertheless, the estimates are sufficiently accurate to indicate the manner in which cesium was distributed. Approximately 57% of the available activity was concentrated in the gas space of the system. An additional 31% was distributed through the hot traps and stainless steel tubing, and the remainder appeared in the stainless steel mesh. Assuming that all the cesium seen in the sodium-filled section was deposited on piping and other surfaces, the stainless steel mesh was an average of 16 times more effective (per unit surface) as a cesium collector than the bare tubing. Considering only the first quarter of the mesh, this effectiveness was increased by another factor of two. (Sodium samples withdrawn from the loop at this time indicated that approximately 10% of the cesium in the sodium-filled section was in solution. However, this does not materially affect the estimated collection efficiencies.) The effectiveness of mesh over tubing as a cesium collector, and the difference in effectiveness among portions of the mesh have not been explained satisfactorily.

The hot traps, representing 27% of the system total wetted surface, were analyzed for ^{90}Sr, ^{137}Cs, ^{144}Ce, ^{155}Eu, ^{60}Co, and Pu. Because the traps were exposed to sodium of varying temperature (Table II), only the

TABLE II

Time-Temperature History of Zirconium Hot Traps

Trap Location	Per Cent of Total Time at Temperature					
	600°C	600-500°C	500°C	500-400°C	400-300°C	<300°C
High temperature leg	57%	18%	--	8%	4%	13%
Low temperature leg	--	--	34%	5%	47%	14%

relative collection efficiency of stainless steel and zirconium and the general effect of temperature on deposition of activity can be obtained. An alcohol rinse was used to remove traces of sodium from each trap, after which the traps were disassembled. Each stainless steel portion (1/3 of the total surface of a trap) and zirconium portion was acid-leached and the leachings were analyzed separately. The results, expressed as activity per square inch of trap material, appear in Table III. The alcohol rinse removed 400 times as much cesium as was recovered by acid leaching, so that the ^{137}Cs values in Table III approach the trivial. Neither ^{144}Ce nor ^{60}Co was detected in the traps.

TABLE III

Fixed Activity Recovered from Zirconium Hot Traps

Specie	Activity Per Unit Surface of Material (β-d/m/in.^{2})			
	High Temperature Trap		Low Temperature Trap	
	Zirconium	Stainless Steel	Zirconium	Stainless Steel
^{90}Sr	9.45×10^4	1.14×10^5	2.96×10^6	4.96×10^6
^{137}Cs	1.30×10^3	1.18×10^3	5.36×10^3	2.16×10^2
^{106}Ru	161	58	below detection	below detection
^{155}Eu†	6.5	1	29.2	31.4
Pu	4.6×10^{-6} mg*	1.51×10^{-6} mg*	4.6×10^{-6} mg*	3.6×10^{-5} mg*

†Quantitative assay was not performed, relative count rates are normalized to ^{155}Eu recovered from stainless steel in the high temperature trap.

*mg/in.^{2}

Concerning the fixed activities (those removed by acid leach, some general observations can be made. Stainless steel is a better strontium collector than zirconium, and stainless steel maintained in the 300-500°C range collected 44 times as much strontium as stainless maintained between 500° and 600°C. Ruthenium appeared only in the hot leg, and at levels suggesting that the fraction of the inventory released from the fuel was negligible. Plutonium was concentrated (by a factor of 24) in low temperature regions on stainless steel, a tendency that has been observed before and has been attributed to solid solution formation. Europium was concentrated equally well by both materials in the low temperature leg. Considering the traps as a whole, 4 times more europium was recovered from the low temperature leg than from the high temperature leg.

None of these concentration effects is particularly impressive, although collectively they indicate that temperature-dependent precipitation, adsorption, and reaction all may have occurred within the contaminated sodium system.

Following removal of the zirconium hot traps the sodium system was cooled to 110°C; this resulted in some pickup of cesium in both the gas phase and the stainless steel mesh collector. A basket containing rods of spectroscopic grade carbon was immersed in the low temperature leg and the whole loop was operated in the range 110°C to 300°C for 1200 h. The carbon trap collected cesium at the expense of the stainless steel tubing and mesh surfaces until the cesium remaining was below the estimated detection limit of 10^6 d/m/in.^{2} surface. During this same period the cesium activity in the gas phase was reduced approximately 42%. Fig. 3 shows the activity distribution before carbon addition and 700 h later. During this period, the loss of cesium from the gas phase and sodium-wet stainless surfaces agreed within 15% with that activity picked up by the carbon bed.

The carbon trap continued to collect activity for the remainder of the test, but redistribution of activity with the bed began after 800 h. This redistribution may have been real or may have resulted from the

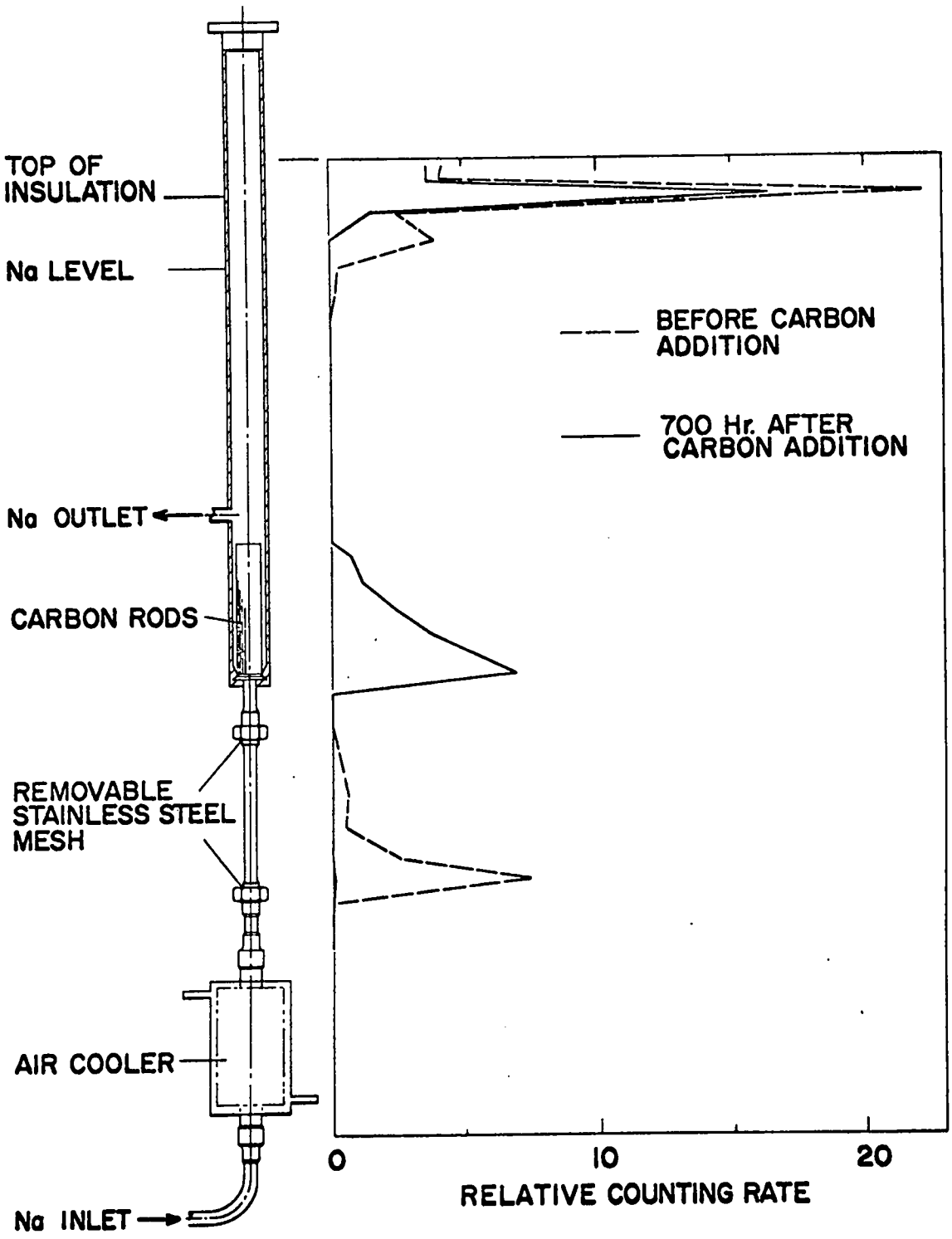

Fig. 3. Effect of Carbon on the Distribution of ^{137}Cs in Low Temperature Leg

combined loss of cesium-bearing carbon particulates from the leading edge and pick up of "new" cesium from sodium. Since the carbon-trapped sodium system was not allowed to approach equilibrium, the long-time stability of cesium adsorbed on the carbon bed could not be determined.

After 1200 h the carbon trap was removed and the stainless steel mesh section was replaced by a full flow sodium oxide cold trap.

C. Results Anticipated During the Next Quarter

The effectiveness of a full flow sodium oxide cold trap in removing long-lived contamination from a sodium system will be evaluated, after which additional irradiated fuel will be placed in the system. A combination of the cold trap, extended surface, low pressure drop mesh packing, and gas phase carbon adsorbers will be used in an attempt to concentrate ^{90}Sr, ^{137}Cs, ^{155}Eu, ^{106}Ru, and Pu released from the fuel.

The addition of a 4096 channel gamma ray spectrometer and tape dump, operating with an available solid state detector, will provide better resolution for study of shorter-lived isotopes than is now possible. Concurrently, trace irradiation of carbide fuel will begin in preparation for study of release and dispersion of activity from these fuels to sodium.

PROJECT 802

MEASUREMENT OF IMPURITIES AND DEVELOPMENT OF QUALITY CONTROL TECHNIQUES FOR HIGH TEMPERATURE SODIUM COOLANT SYSTEMS

Person in Charge: D. B. Hall

Principal Investigators: R. H. Perkins
V. J. Rutkauskas

I. INTRODUCTION

The objectives of this investigation are:

1. Determination of the solubility of oxygen in sodium as a function of temperature using the vacuum distillation analytical technique.
2. Development of dynamic in-line sodium sampling techniques for the vacuum distillation analytical method. The intent of this phase of the program is to develop a prototype sampling system capable of extracting representative sodium samples from engineering systems for the analysis of all dissolved impurities, including fission product elements. With minor modification this sampling system will have the capability of being used in a radioactive sodium environment.
3. Development and evaluation of prototype in-line analytical instrumentation for the continuous monitoring of oxygen and/or gaseous and metallic impurities of interest in sodium systems.
4. Evaluation of the (n, γ) activation technique for the determination of oxygen and carbon in sodium and other activation analytical techniques for impurities in sodium.
5. Evaluation of the lowest oxygen levels which can be practically maintained for the cold trap and hot trap mode of quality control.

6. Development and evaluation of techniques utilizing soluble "getters," i.e., magnesium, calcium, and barium as quality control mechanisms for maintaining system oxygen concentrations, and the development of analytical methods required to evaluate and monitor this particular mode of quality control. This technique has the potential for effectively controlling not only oxygen, but carbon, hydrogen, nitrogen and possibly metallic fission product elements and other metallic impurities.

II. IMPURITY ANALYSIS AND SAMPLING STUDIES

(V. J. Rutkauskas)

A. Status of Work in Progress

The solubility of oxygen in sodium using the vacuum distillation analytical technique was evaluated over the temperature range of 124°C to 300°C. The results obtained at the lower temperatures indicate that the solubility of oxygen in sodium at these temperatures is much lower than previously published data. The reproducibility of results obtained at each of the equilibrium temperature conditions was excellent with an apparent standard deviation of 0.5 ppm in the oxygen concentration range of 1 to 10 ppm and 5% above 10 ppm. The data obtained from this investigation are shown in Table I.

A dip-type, full flow, vacuum distillation sampling system for dynamic in-line sodium sampling and analysis has been designed, fabricated, assembled and bench tested preparatory to being installed in the sodium analytical loop No. 1 for testing and evaluation.

A dynamic facility incorporating an integral sampling and sample transfer chamber for the evaluation of analytical methods for the determination of carbon in sodium in the range of 1 to 10 ppm has been designed.

Preliminary design of the experimental facility (analytical loop No. 2) to investigate the areas of development described in Items 3, 5, and 6 under Project Objectives has been initiated. A flow model of the system mixing chamber has been fabricated and assembled and is currently undergoing test.

TABLE I

Solubility of Oxygen in Sodium

	Temperature, °C											
	125	150	165	175	185	200	215	225	250	265	275	300
Oxygen Concentration (ppm)	1.7*	2.3	4.0	4.9	6.8	8.1	10.6	21.9	37.1	46.5	74.4	145.9
	1.7*	2.5	4.6	4.9	6.8	9.0	11.6	20.1	40.1	48.7	72.3	134.5
	2.3*	2.3	3.3	5.0	7.2	7.9	11.2	18.5	37.8	49.2	74.3	145.3
	2.5*	2.0	3.7	4.6	7.5	9.5	13.1					
	2.2*			5.4	6.3							
	1.7*				6.7							
	1.7											
	1.4											
	1.4											
	1.2											
Average Concentration (ppm)	1.8	2.3	3.9	5.0	6.9	8.6	11.6	20	38	48	74	142
Standard Deviation (ppm)	.4	.2	.5	.3	.4	.8	1.0	2	2	1	1	6
Relative Standard Deviation (%)	22	9	13	6	6	9	9	10	5	2	1	4

*Initial samples taken during preliminary system checkout.

B. Plans for Second Quarter, FY '67

The dip-type, full flow, vacuum distillation sampling system will be installed in the sodium analytical loop No. 1 where it will be rigorously tested and evaluated against the integral sampling system presently installed in the facility.

The off-gases associated with the vacuum distillation method for the analysis of oxygen in sodium will be studied to determine the quantity and composition of the gases. This information is necessary in order to evaluate the problems, if any, associated with the time and temperature of distillation on the nature of the residues and to determine if this technique is applicable for the determination of carbon in sodium.

The sodium sampling and sample transfer techniques for the (n,γ) activation analysis technique will be evaluated and equipment designed, modified and/or fabricated for the first series of (n,γ) evaluation experiments which will be performed with ~25 ppm oxygen in sodium.

Work will continue on the design of the analytical loop No. 2 experimental facility. The mixing chamber model tests will be concluded and the information obtained from this test will provide the necessary design parameters for this portion of the facility. Equipment procurement and fabrication will be initiated as the design progresses.

C. Plans for Future Work

Investigation into the problems associated with sodium sampling and analysis of impurities in sodium will continue with the objective of developing a prototype sampling system for engineering systems and reactor plant application and the development of in-line analytical techniques and alternate analytical techniques to complement the vacuum distillation analytical technique.

The first series of experiments planned for analytical loop No. 2 will be to evaluate the LASL dc electrical resistivity meter and the United Nuclear electrochemical cells as a function of oxygen concentration and sodium temperature using the vacuum distillation analytical technique as a primary standard. This work will extend the earlier studies at similar instruments.

Studies on solution gettering with calcium, magnesium, and barium will be initiated. This will require development of analytical methods, solubility and temperature relationships and techniques for introducing and maintaining the desired metallic concentrations as well as mechanisms for removing the metallic and depleted metallic getter.

PROJECT 803

KINETICS OF SODIUM COLD TRAPS

Person in Charge: D. B. Hall

Principal Investigators: R. H. Perkins
C. C. McPheeters

I. INTRODUCTION

Control of oxygen concentration in liquid sodium can be accomplished by precipitating sodium oxide at low temperature in a cold trap. The purpose of this study is to define and measure the parameters necessary for effective design of cold traps. The design parameters will be determined from data obtained with experimental cold traps. The behavior of cold traps will be studied under transient conditions; data obtained will be used to formulate a valid theoretical description of the mechanism and parameters which control the the precipitation of sodium oxide. Once the appropriate parameters have been measured, an engineering approach to cold trap design will then be possible.

II. COLD TRAP KINETICS

(C. C. McPheeters, J. M. Williams)

A. Considerations in Experiments with Cold Traps

The application of engineering analysis to the design and performance prediction of cold traps as oxygen removal devices in sodium systems has been nonexact. Optimum design of a cold trap requires a much more detailed analysis of the basic mechanisms which characterize cold trap operation. The concept of a cold trap implies transporting a sodium stream down a temperature gradient into an isothermal volume which is the coldest point in the system. At steady state, all oxygen present in the

system (other than dissolved oxygen and oxygen associated with system surfaces) is in the isothermal volume. During cleanup operations, sodium oxide precipitates somewhere in the region where the temperature gradient exists. For proper design to prevent flow blockage in the temperature gradient region, it is necessary to know the rate at which the solid phase precipitates in this region. Since the temperature gradient region is generally arranged as an economizer heat exchanger, it can be seen that in designing it, there are conflicting requirements between the need for heat transfer surface on one hand and non-blockable flow channels on the other.

The cold trap design to be used in this study is a compromise between heat transfer requirements, possible flow blockages and simplicity. Simplicity of design is necessary because of the difficulty of mathematically correlating cold trap performance with cold trap geometry. Design and operating variables to be studied include cold trap volume, internal surface area (wire mesh packing), flow rate, oxygen concentration range and temperature distribution. Six different cold traps will be tested during this program. These six cold traps will cover an array of the two geometrical variables of volume and internal area. The same basic design will be common to all the cold traps, and the variations in volume will be made while maintaining a constant length to diameter ratio for the cold trap components. The first cold trap to be tested and the largest of the series will be constructed of an outer tube 4 in. x 0.125 in. wall thickness x 35 in. long; an inner tube 2 in. o.d. x 0.030 in wall thickness x 30 in. long will define the annular flow channel. The cold trap will be cooled with NaK (in an outer jacket). Sodium will enter the cold trap annulus at system temperature. As the sodium progresses along the annulus, it will be cooled, and at the point where the sodium becomes saturated with oxygen, sodium oxide precipitation will begin. The initial assumption will be that all sodium oxide precipitation occurs on surfaces. Precipitation in the bulk liquid has a much lower probability; however, the latter will be considered. Later analysis of the data will, it is hoped,

determine which mechanism is dominant and to what degree each is present. Precipitation will continue until the coldest point in the cold trap is reached. The sodium then will leave the cold trap via the central tube.

The following mathematical analysis is given only to demonstrate the type of analysis to be used in this study. A more detailed analysis will be performed later in the program. Possible consequences of liquid phase precipitation of sodium oxide will be considered in the more detailed analysis.

Consider an incremental section of the cold trap at some distance, x, from the entrance to the annulus. The rate of oxygen entrance into the segment, R_1, is equal to the sum of the rate of oxide precipitation on the wall, R_2, and the rate of oxygen passage out of the segment, R_3,

$$R_1 = R_2 + R_3 \tag{1}$$

Expressing these rates in terms of flow, precipitation rate constant, concentration and surface area in appropriate units, we obtain

$$WC = KP(C - Ce)\, dx + W(C + dC) \tag{2}$$

where

W = sodium flow rate

C = oxygen concentration in the sodium at x

C + dC = oxygen concentration in the sodium at x + dx

K = oxide precipitation rate constant

P = total annulus perimeter

Ce = equilibrium oxygen concentration based on the sodium temperature at x.

Equation (2) can be reduced to

$$\frac{dC}{dx} = \frac{KP}{W}(C - Ce) \,. \tag{3}$$

It can be seen from mass balance requirements that

$$\frac{dCs}{dt} M = W\,(Cs - Co) \,, \tag{4}$$

where

Cs = system oxygen concentration

t = time

M = system mass

W = sodium mass flow rate

Co = cold trap exit oxygen concentration.

The equilibrium oxygen concentration, Ce, in Eq. (3) is a function of temperature, and the temperature profile along the cold trap length is a function of flow rate. The temperature profile will be measured during the cold trap operation.

The precipitation rate, K, in Eq. (3) will be determined and any variation in K due to changes in flow rate, cold trap volume, system oxygen concentration, internal area or temperature distribution will be studied. Some details of the sequence of experiments and measurements are given in the following section.

B. Plan of Experiments

The cold trap test loop will be an isothermal, forced convection sodium system which will consist of a ballast tank, a cold trap section and associated piping, expansion tank and NaK coolant circuit. The sodium will be pumped from the ballast tank to an analytical section where a United Nuclear Corporation (UNC) oxygen meter, a vacuum distillation sampler and a plugging indicator will be used to analyze the sodium for oxygen. From the analytical section, the sodium will pass through the cold trap to an expansion tank. The expansion tank will be used as a heat input section and an impurity addition system. The sodium will then flow through a second UNC oxygen meter back to the ballast tank. A NaK coolant circuit will be used to remove heat from the cold trap and to dump the heat to air.

Data from six cold trap designs will be obtained by the following procedure:

1. Establish constant, well defined conditions of flow rate, oxygen concentration and cold trap temperature distribution, then let the system oxygen concentration come to equilibrium.
2. Isolate the main portion of the system from the cold trap section while allowing constant flow through the cold trap.

3. Change the cold trap temperature distribution to a new condition -- either higher or lower.
4. When the new cold trap temperature distribution is well established, allow sodium from the main system to again flow through the cold trap.
5. Take oxygen concentration data as a function of time both at the entrance and at the exit of the cold trap.

The data obtained by this procedure will be used to establish a model of the mechanisms of cold trap operation.

C. Status of Work in Progress

During the current reporting period, the sodium test loop has been designed, and the detail drawings are now in progress. The drafting details are estimated at approximately 60% complete. Many of the components to be used in this loop are on hand. (These components were originally built for use in the Fast Reactor Core Test Facility (FRCTF) sodium system.) These components include:

1. 65 gal tank 18 in. diam with 0.250 in. wall thickness stainless steel type 304.
2. Two Mine Safety Appliances ½ in. electromagnetic sodium pumps.
3. Five 1 in. globe-type bellow-sealed valves.
4. All necessary 1 in. stainless steel type 304 pipe.

Miscellaneous items such as the tank support structure, sodium catch pan, NaK cold trap cooler air heat exchanger and level probe seals have been made and are on hand.

Actual construction of the loop is scheduled to begin in November when space for the loop will become available as a result of building modifications.

A computer program for predicting the temperature profile and concentration gradients in this cold trap geometry is being studied. The FORTRAN IV code for this study is now capable of predicting temperature profiles as a function of flows, boundary temperatures and geometrical designs.

Future expansion of the code will be directed toward the prediction of oxygen concentration gradients.

D. Plans for Second Quarter, FY 1967

Construction of the test loop will be started and should progress to the stage of trace-heater installation during the next reporting period.

The FORTRAN IV computer code will be improved to include prediction of concentration gradients in the cold trap.

PROJECT 807

CERAMIC PLUTONIUM FUEL MATERIALS

Person in Charge: R. D. Baker

Principal Investigator: J. A. Leary

I. SYNTHESES AND FABRICATION

(R. L. Nance, M. W. Shupe, W. C. Pritchard, T. K. Seaman)

1. Oxides

Powders of PuO_2 are prepared routinely by calcination in air of plutonium(III) oxalate or plutonium(IV) peroxide. Results of studies on powder comminution, pressing, and sintering have been reported.[1] The major conclusions from this study were

(a) Single phase PuO_2 pellets having densities as high as 97% of theoretical can be produced by sintering cold pressed pellets at 1250 to 1500° C.

(b) Sintering PuO_2 in non-oxidizing atmospheres results in a two phase material that contains α-Pu_2O_3 in PuO_{2-x}.

(c) Addition of 0.5 w/o paraffin binder produced less dense pellets than pellets pressed and sintered without binder.

Formation of α-Pu_2O_3 in PuO_2 sintered in non-oxidizing atmospheres can be prevented by adding a few volume percent of Mo or W metal powder, as shown in Table I. The lattice parameter of the PuO_2 phase sintered with Mo was always significantly lower than that of the 100% PuO_2 specimen.

Table I

Effect of Metal Powder on PuO_2 Pellets Sintered for 4 hr. at 1650°C in Ar

Metal Powder		α Pu_2O_3 in Pellet	PuO_2 Lattice Constant, A
Type	v/o		
(none)		yes	5.3955
Mo	2	no	5.3940
(none)		yes	5.3953
Mo	5	no	5.3946
(none)		yes	5.3953
Mo	10	no	5.3945
(none)		yes	5.3951
W	0.30	yes	5.3977
(none)		yes	5.3951
W	1.20	no	5.3949

2. Carbides

Carbide compositions $PuC_{0.86}$, UC, (U, Pu)C, Pu_2C_3, $(U, Pu)_2C_3$, and $(U, Pu)C_2$ have been synthesized. These compositions are prepared by comelting the elements in an arc furnace. The resulting material is then solution treated, pulverized, cold pressed, and sintered into pellets for properties measurements. In the case of monocarbides $PuC_{0.86}$ and $U_{0.8}Pu_{0.2}C$, the ingots also have been directly cast into rods and solution treated.

3. Nitrides

Single phase PuN has been prepared routinely by reaction of partially hydrided electrorefined Pu metal with N_2. The procedure has been described in detail.[2]

Analysis of the most recently prepared lot (PuN-13) is shown in Table II.

Table II

Analysis of Lot PuN-13 (100 g. scale)

Pu analysis, theoretical w/o	94.47
Pu analysis, found	94.47 ± 0.01
N analysis, theoretical	5.53
N analysis, found	5.49 ± 0.04
lattice parameter	4.9051 ± 0.0002 A

Uranium mononitride is prepared by thermal decomposition of uranium sesquinitride at 1500°C in argon.

Solid solutions of UN and PuN are prepared by blending ball milled UN and PuN powders followed by cold compaction and sintering. Results of sintering in N_2 at 1900°C are shown in Figure 1. There is a slight negative deviation from Vegard's Law at low concentrations of PuN, and a slight positive deviation at higher concentrations. Identical results are obtained when pressed pellets of mixed UN and PuN powders are sintered in argon at 1600°C.

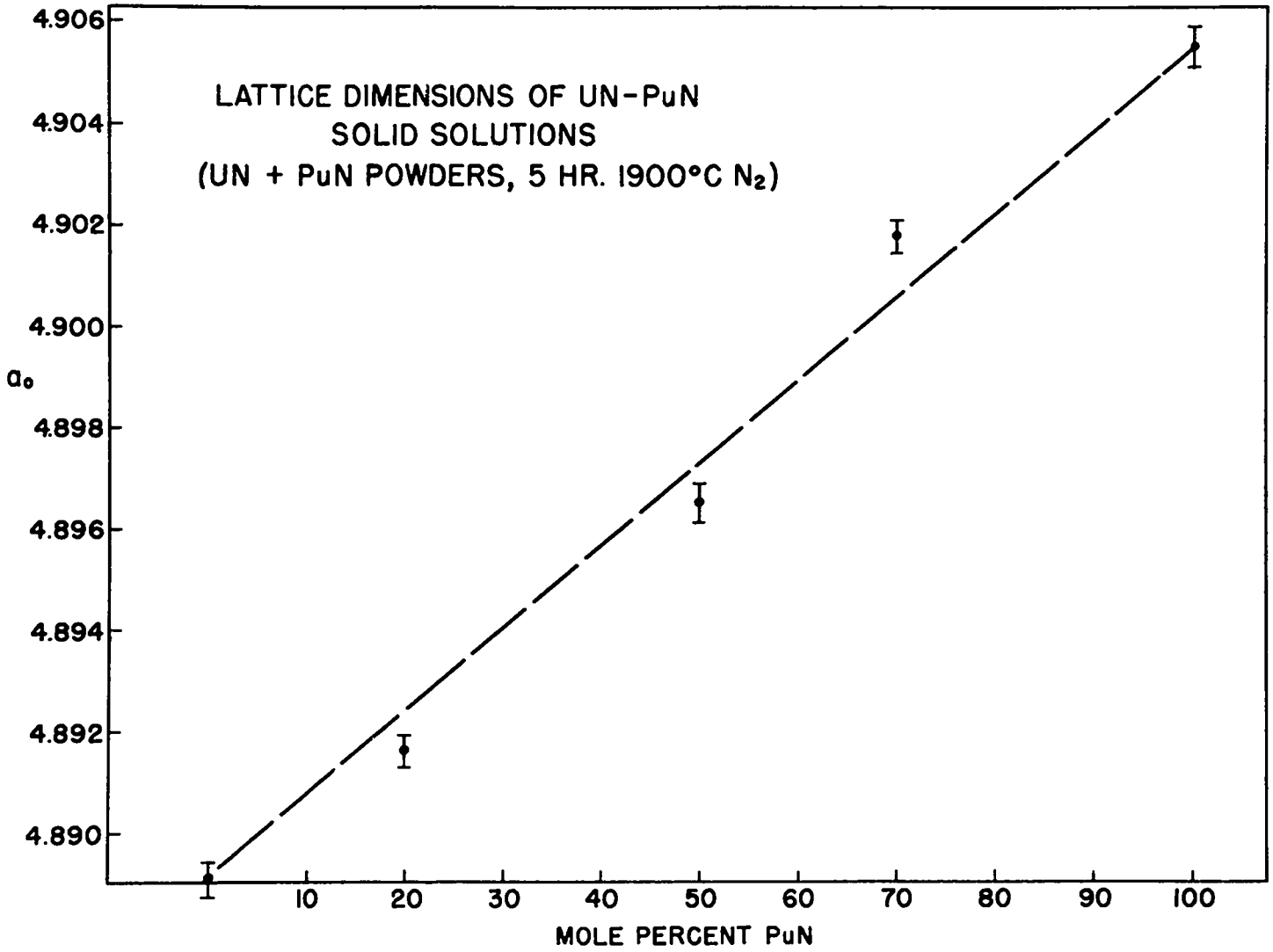
LATTICE DIMENSIONS OF UN-PuN
SOLID SOLUTIONS
(UN + PuN POWDERS, 5 HR. 1900°C N2)
4.906
4.904
4.902
4.900
a0
4.898
4.896
4.894
4.892
4.890
10
20
30
40
50
60
70
80
90
100
MOLE PERCENT PuN

Fig. 1

The results of pellet pressing and sintering studies on PuN and (U, Pu)N, Pu(N, O) and Pu(C, N) have been reported.[3] Generally the nitrides do not sinter to very high densities under normal conditions. However, high densities can be achieved if the powder particle size is sufficiently small. Typical results obtained with PuN are shown in Table III. Microstructure and x-ray powder diffraction analysis indicate that the sintered material is single phase PuN.

Table III

Densification of PuN Powder after 100 hr. Ball Milling (Size distribution: 85% ≤ 2 μ, 13% 2-5 μ by count). Sintered 4 hr. at 1800°C in Ar

Pressing Pressure, t. s. i.	Pellet Density, % Theor.	
	Unfired	Sintered
40	69. 1	94. 8
60	70. 6	95. 0
80	71. 2	95. 1

II. PROPERTIES

1. Differential Thermal Analysis (J. G. Reavis)

Phase relationships in the Pu-C, U-Pu-C, Pu-N, and U-Pu-N systems are being studied by DTA. The instrument is capable of detecting transitions in plutonium materials in either vacuum or inert atmospheres. Temperatures of greater than 3000° C are attainable. The apparatus is a modified version of a previously described[4] DTA unit.

In general high temperature measurements in the specialized equipment required for plutonium materials are subject to greater errors than with normal materials. Therefore an intensive temperature calibration study was undertaken. Calibration points are shown in Table IV. The uncertainties assigned to each temperature indicate the reproducibility that is attainable on reassembly of the furnace with different specimens of the same material.

Table IV

Calibration of DTA Instrument

Transition	Temperature, °C	
	Literature	Observed
Cu, m.p.	1083	1080 ± 10
Pt + C, m.p.	1734	1735 ± 10
Pt, m.p.	1770	1760 ± 10
UC_2, tet.-cubic	1765	1765 ± 10
Rh, m.p.	1970	1970 ± 20
Ir, m.p.	2440	2440 ± 20
$MoC_{0.2}$ eutectic	2205	2200 ± 10

Pu-C System: This system is not well characterized at high temperatures in the region 50-100 atom percent C. Therefore analysis of several compositions have been done in conjunction with x-ray powder diffraction and metallography. Although results are incomplete, the transitions shown in Table V have been verified by both cooling and heating curves.

Table V

Transitions Observed by DTA in the Pu-C System

Composition, a/o C	Transition Temperature, °C. 1st.	2nd	3rd
61	1650	1980	
64	1650	1980	
67	1640	none	2210
70	1645	none	2220
80	1650	none	2230
90	1645	none	2230

The first transition probably is the $Pu_2C_3 + C \mid PuC_2$ transition, reported to be at $\sim 1750°$.[5]

The second transition at 1980°C. is presumably the melting of Pu_2C_3, based on metallographic examination of the material after solution treating at 1990°C. This melting point is 70° below the reported value. The third transition at 2220 is in fairly good agreement with the melting point of ~ 2250 reported for PuC_2.[5]

U-Pu-C System: Ternary compositions that have been examined to date are shown in Table VI. The first transition observed in the high carbon compositions probably represents the $M_2C_3 + C/MC_2$ transition, which occurs at 1650° in the Pu-C system and at $\sim 1500°$ in the U-C system.[6] The transition at $\sim 2330°$ probably is related to melting of MC_2, which occurs at 2220° in the Pu-C system and at $\sim 2450°$ in the U-C system (eutectic at $\sim UC_{2.05}$).

Table VI

Transitions Observed by DTA in the U-Pu-C System

Composition	Transition Temp., °C	
	1st	2nd
$U_{0.5}Pu_{0.5}C_2$	1745	2325
$U_{0.5}Pu_{0.5}C_4$	1745	2340
$U_{0.8}Pu_{0.2}C$		2465

Nitrides: Preliminary results indicate that no transitions are detectable when PuN or $U_{0.8}Pu_{0.2}N$ are heated to 2300° under 0.5 atm. nitrogen.

2. X-ray Powder Diffraction (C. W. Bjorklund, R. M. Douglass, R. L. Nance)

In addition to powder diffraction studies on uranium-plutonium fuel materials, work is continuing on the self-irradiation damage to various plutonium ceramics. Recoil atoms produced by the α-disintegration of plutonium cause the displacement of atoms to interstitial sites with a consequent expansion of the lattice. The extent of self-irradiation damage is being determined by measuring the increase in the lattice parameters of the compounds as a function of time. Debye - Scherrer x-ray photographs were obtained with 114.6-mm. -diameter powder cameras using nickel-filtered copper Kα radiation. Between exposures the compounds were stored without removal from the glass or quartz capillaries in order to minimize effects due to sampling, etc. Lattice parameters were calculated from measurements of high angle reflections using the Nelson-Riley extrapolation to correct for absorption.

Compounds of "normal" isotopic composition, i.e., ~95 atom % Pu-239, currently being studied include the following (sample ages in days are given in parentheses); PuO_2 (1096), PuN (949), PuN (402), and Pu_2C_3 (366). In addition,

a number of compounds have been prepared in which the Pu-238 content has been increased to ~ 4.0 atom percent with a resultant 10-fold increase in total energy deposition. These include $PuC_{\sim 0.86}$ (242 d), PuC and Pu_2C_3 phases in equilibrium (duplicate samples, 157 days), PuO_2 (834), and duplicate samples of PuO_2 (ranging in age from 344 to 581 days) stored at temperatures between -200° and +400°C.

To facilitate comparison, results have been expressed in the form $\Delta a/a$ as a function of time. To date, the rate of lattice expansion has been found to increase in the order $Pu_2C_3 < PuN < PuO_2$ for compounds of normal isotopic composition, and Pu_2C_3 (in equilibrium with PuC) $< PuC_{0.86} < PuO_2 < PuC$ (in equilibrium with Pu_2C_3) for compounds containing added Pu-238. The lattice parameters of the compounds of normal isotopic composition continue to increase at a steady rate whereas those of the latter series have nearly all levelled off, perhaps asymptotically. A striking exception is observed in the case of PuC in equilibrium with Pu_2C_3, for which the value of $\Delta a/a$ is more than half again as large as that of PuO_2 and is still increasing. Preliminary curve-fitting calculations have been made but are still subject to change as additional data are obtained. No evidence of line-broadening has been observed for any of the compounds

3. High Temperature X-ray Diffraction (J. L. Green, A. L. Gonzales)

The high temperature furnace attachment for the Picker diffractometer, capable of a design temperature of 2500°C., is being fabricated.

4. Neutron Diffraction (J. L. Green)

Neutron diffraction studies on uranium and plutonium materials are being conducted. From these results the following information can be obtained.

(a) basic crystallographic data

(b) phase relationships

(c) Magnetic ordering phenomena of use in solid state theory

(d) Thermal expansion as a function of temperature

Experimental work using available neutron diffraction equipment has continued. During this period, it was possible to complete a preliminary determination of the crystallographic atomic position parameters for Pu_2C_3. An appropriate target of carbon-rich Pu_2C_3 was prepared and the diffraction pattern of this material was recorded at room temperature. Reflection intensity information derived from these data allowed preliminary values for the position parameters for both Pu and C to be computed. The position parameter for Pu was found to be 0.050 ± 0.002 which is in excellent agreement with the value of 0.050 ± 0.003 as determined by Zachariasen from x-ray data. The carbon parameter was found to be 0.289 ± 0.004. Considerable difficulty was caused by the large fast neutron background derived from the thermal fission of the Pu^{239} in the target. Because of this problem, quantitative information was obtained for only 12 reflections. For this reason, a supply of enriched Pu^{240} has been obtained for use in future measurements of this sort. The thermal fission cross-section for Pu^{240} is only ~ 100 mb; therefore, the peak to background ratios for targets prepared from this material are more favorable than for Pu^{239} by approximately an order of magnitude. A $^{240}Pu_2C_3$ target is presently being prepared to allow a final determination of the position parameters for this compound to be made.

It has been suggested in the literature that an antiferromagnetic transition might occur in PuC at a temperature of from 20 to 100°K. Low temperature neutron diffraction measurements have been undertaken to determine whether or not this transition in fact occurs. In preliminary neutron diffraction studies no transition was observed. However, the target was prepared from plutonium of normal isotopic composition, and the incoherent fast neutron background

was excessive. The experiment is now being repeated using a target prepared from ^{240}Pu C. Data collection is still in progress.

Equipment is now being fabricated to extend the temperature range of neutron diffraction on plutonium specimens to $\sim 2500^{\circ}$C.

5. Thermodynamic Properties from EMF Cells (G. M. Campbell and L. J. Mullins)

For electrochemical EMF measurements to be useful in calculating thermodynamic properties the electrochemical cell must be at a thermodynamic equilibrium. It is not always easy to tell when such an equilibrium is obtained, especially when the reactions involved are slow, as is usually the case when solid compounds are used as electrodes. Also, since Pu is a very active metal there are apt to be side reactions producing a mixed potential in any cell that contains it. Therefore, the electrolyte must have no components that react with Pu metal at the temperature of the measurement. Fused LiCl-KCl eutectic is a satisfactory electrolyte when properly purified.

To gain experience in the preparation of this electrolyte as well as to characterize the Pu metal electrode in it, the first cell studied was

$$Pu\,|\,Pu^{+3}\,(x_1),\ LiCl\text{-}KCl\,||\,LiCl\text{-}KCl,\ Ag^{+}\,(x_2)\,|\,Ag \qquad (I)$$

at 685 to 730°K. The Ag electrode was constructed so that it could be reproduced closely from one cell to another. This made it possible to incorporate the electrode in the cell

$$Ag\,|\,Ag^{+}\,(x_2)\ LiCl\text{-}KCl\,|\,Cl_2, C \qquad (II)$$

and indirectly determine the EMF of Pu versus Cl_2.

The EMF's were found to fit the Nernst equation, after a small correction for the junction potential, where x_1 ranged from 0.059 to 2.15 mole percent. By combining the results of the cells (I) and (II) the Gibbs standard free energy of formation (ΔG°) of $PuCl_3$ in NiCl-KCl eutectic in the concentration range measured was calculated to be

$$\Delta G^\circ_T = -224 + 0.046\ T \qquad \text{(kcal/mole)}$$

We feel these results show that the Pu electrode does reach a reversible equilibrium in LiCl-KCl electrolyte.[7]

Nitrides: The cell

$$N_2(g_1 p_1),\ PuN(s)\ |\ Pu^{+3}\ (x_1)\ LiCl\text{-}KCl\ ||\ LiCl\text{-}KCl,\ Ag^{+}\ |Ag \qquad \text{(III)}$$

has been measured over the temperature range 695 to 716°K and the composition range $x_1 = 0.0177$ to 0.0193 mole fraction.[8] It was known that N_2 reacts with Pu at this temperature and an attempt was made to prepare a PuN electrode in situ. The mechanical properties of this electrode were unsatisfactory. Sintered pellets attached to a Ta rod were found to provide a satisfactory electrode.

The cells behaved in a reversible manner; i.e., the EMF was independent of the direction of temperature approach and obeyed the Nernst equation with respect to nitrogen pressure and Pu^{+3} concentration, x_1. The EMF was independent of time after an initial 24-hr cell equilibration period.

Combining the results from cells of types (I) and (III) and correcting the EMF data of cell (III) to a nitrogen pressure of 1 atm gave the standard free energy of formation as

$$\Delta G^{\circ}_{T} = -99 + 0.055\ T \qquad \text{(kcal/mole PuN)}$$

The data for type (III) cells were obtained over a temperature range of about 21°. Therefore, standard heat and entropy terms derived from these data cannot be considered reliable. By using a reasonable estimate of the entropy change for this reaction of $\Delta S^{\circ}_{298} = -22$ the heat of formation $\Delta H^{\circ}_{298} = -76$ kcal/mole was estimated from the EMF results.

Carbides: Several carbide cells of the type

$$Pu \,|\, Pu^{+3},\ LiCl\text{-}KCl \,|\, Pu_2C_3 + C \qquad \text{(IV)}$$

$$PuC,\ Pu_2C_3 \,|\, Pu^{+3},\ LiCl\text{-}KCl \,|\, Pu_2C_3 + C \qquad \text{(V)}$$

$$Pu(s) \,|\, Pu^{+3},\ LiCl\text{-}KCl \,|\, Pu_2C_3 + PuC \qquad \text{(VI)}$$

have been measured in the temperature range 753° to 879°K. Preliminary results indicate that at 800°K, ΔG° (Pu_2C_3) is about - 63 kcal/mole and ΔG° (PuC) might be as negative as - 28 kcal/mole. However, additional measurements are needed at higher temperature.

In order to overcome some of the problems associated with a liquid plutonium reference electrode, a secondary reference ($PuRu_2 + Ru$) is being measured. Preliminary results indicate that this reference electrode behaves reversibly at temperatures up to 1055°K.

A second approach to achieving higher temperature cells for refractory fuel materials involves the use of a solid electrolyte.

Measurements on the cell

$$Pu\text{-}PuCl_3(s) \mid BaCl_2(s) \mid NaCl\text{-}AgCl, Ag^{(s)} \qquad (VII)$$

have yielded tentative values for the Gibbs standard free energy of formation of $PuCl_3$ over the temperature range 500 - 560°C. The EMF values range from 1.713 volts at 500°C to 1.700 volts at 560°C. These values when combined with the data for the cell[9]

$$Ag(s) \mid AgCl,\ NaCl\ (s) \mid Cl_2\ (g)$$

give standard free energy of formation values of -185 kcal/mole $PuCl_3$ at 500°C and -182 kcal/mole at 560°C.

6. Thermodynamic Properties from Vaporization Studies (R. A. Kent)

Although the use of Knudsen technique to measure vapor pressures and heats of sublimation is well established, vaporization processes at high temperatures are often complex and a detailed knowledge of the identity and relative concentrations of the vapor species is required if the vaporization process is to be characterized. The use of a mass spectrometer in conjunction with the Knudsen technique allows one to identify the vapor species and to determine their relative amounts at the same time one measures the vapor pressure and heat of sublimation.

The high temperature mass spectrometer assembly for plutonium materials that has been constructed is shown in Fig. 2. The unit consists of two basic components, an oven assembly incorporating an electron bombardment - heated Knudsen cell, and an Ultek Corporation Model 200 quadrupole residual gas analyzer which has been modified to produce the highly controlled ionizing beam necessary for quantitative measurements. These component parts are contained in a differentially pumped stainless steel vacuum envelope. Vacuum of the order of 10^{-8} torr is achieved by means of two ion pumps, one rated at 400 ℓ/s connected to the quadrupole region, the other rated at 100 ℓ/s connected to the oven region.

The molecular beam which effuses from the Knudsen cell passes through a collimating slit in a movable shutter plate and into the quadrupole region. The movable shutter plate allows one to close the slit to the molecular beam so as to distinguish sample vapors from background species.

The mass spectrometer consists of three parts, an ionizer region, a quadrupole analyzer region, and a detector consisting of an electron multiplier with a gain of about 10^5. When molecules enter the ionizer region they pass through a beam of electrons of known energy and positive ions are formed according to the equation

$$M + e^- = M^+ + 2e^-$$

while other reactions can and do occur, this reaction is the important one in these investigations. The positive ion beam is focused and accelerated into the quadrupole analyzer region. The signal from the multiplier can be fed either to an oscilloscope or through an electrometer to a strip chart recorder.

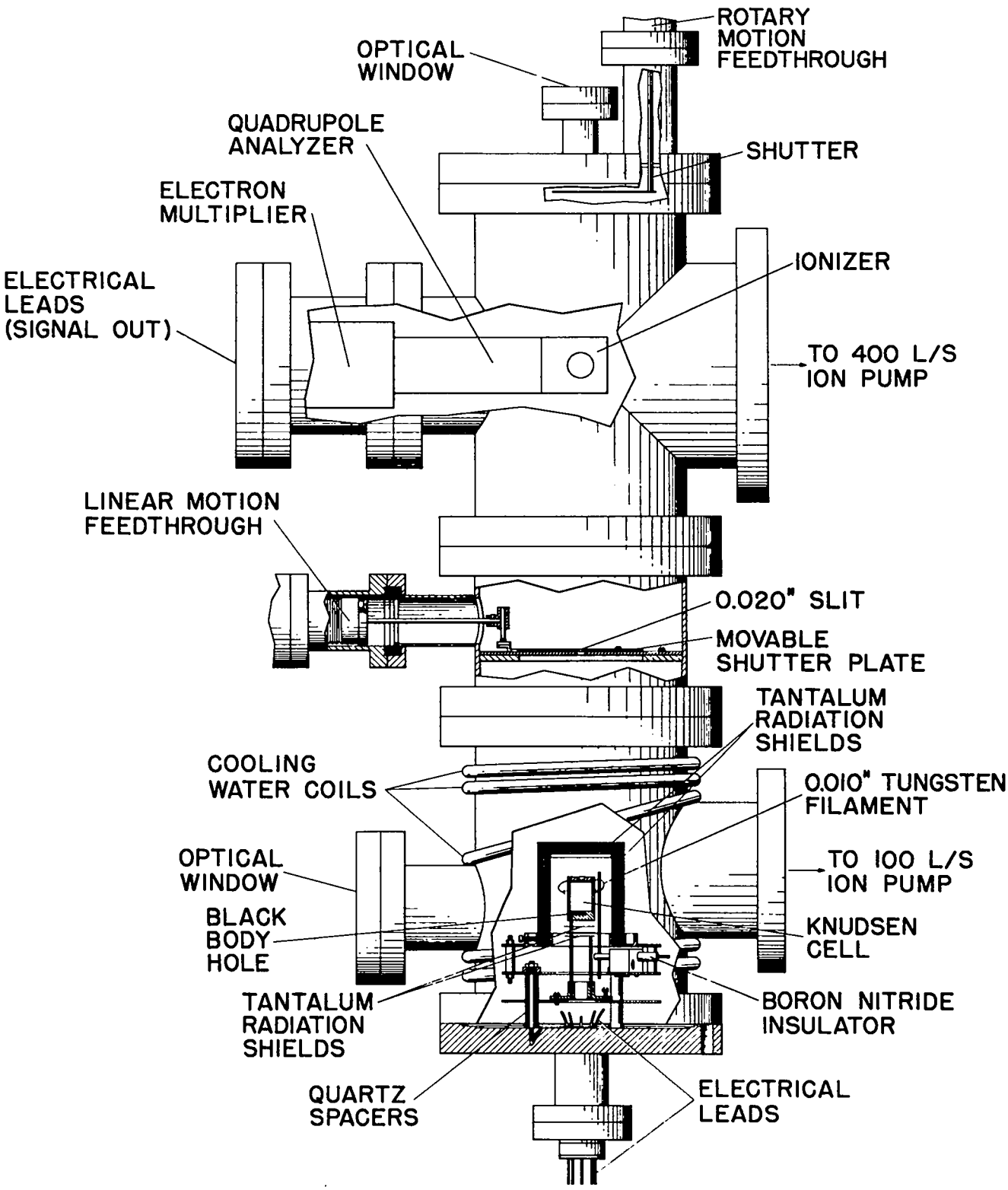

Fig. 2. Knudsen Cell and Vapor Analyzer

This type of measurement permits one to determine quantitatively the identity and the partial pressures of vapor species above plutonium compounds at high temperatures and the heats of sublimation of these species. In addition, when these data are combined with data available from other experiments the heats of formation of both condensed and vapor species and the dissociation energies of the vapor species can be calculated

7. High Tempeature Calorimetry (A. E. Ogard)

A high temperature "drop" calorimeter suitable for measuring changes in enthalpy of plutonium-containing compounds has been constructed. The apparatus is based upon the design of Southard[10] in which an encapsulated sample is heated in a furnace to a known temperature and then is dropped into a massive calibrated copper calorimeter block. The furnace is capable of attaining 2900°C with slightly less than 1 atmosphere of Argon in the furnace and calorimeter. The lid of the capsule is welded shut with approximately 1/3 atmosphere of helium or argon in the capsule. In the temperature range of 900° to 2100°C the capsule is suspended in the furnace by means of a 0.030 in. dia. tungsten wire. This suspending system is built so that repeated drops and heatings can be made without dismantling the furnace or calorimeter. Above 2100°C a graphite rod is used to hold the capsule and is broken for each drop.

The apparent heat content above 25°C of an empty tungsten capsule, supplied by GE-APO, has been determined in the temperature range 1000 - 2100°C. The results are compared with literature values in Table VII.

Table VII

Apparent Heat Content of Tungsten Capsule (GE-San Jose #3)

Temp., °C	$H_T - H_{298}$, cal/g		
	This Work	Ref. 11	Ref. 12
1048	35.5	35.6	
1080	36.4	36.5	
1146	40.2	39.0	
1275	45.1	43.7	
1330	47.2	45.7	
1537	54.8	54.0	
1560	56.3	54.8	
1760	64.2	62.7	
1960	72.2	70.8	72.2
2065	77.3	75.2	77.2

It should be emphasized that only the apparent heat content has been determined in these experiments. During the drop some heat is radiated to the surroundings before the capsule enters the calorimeter, and some heat is conducted by the suspending wire from the furnace to the calorimeter. Corrections have not been made for these heat transfers in order to obtain the true heat content. The apparent heat content of the tungsten capsule will be subtracted from the heat content of the loaded capsules to arrive at the true heat content of the materials in the capsule. As soon as capsules filled with UO_2-PuO_2 solid solutions are received, measurement of the heat content of $(U, Pu)O_{2\pm x}$ will begin. The temperature range of the experiments will also be extended to $\sim 2900°C$.

8. Thermal Conductivity (R. L. Thomas)

At the present time there is very little information available on the thermal conductivity of plutonium ceramic fuels. Results have been reported[13] for UC, $U_{0.9}Pu_{0.1}C$, $U_{0.8}Pu_{0.2}C$, $U_{0.7}Pu_{0.3}C$, and $PuC_{0.87}$ in the temperature range 200-400°C. More recently the data for $U_{0.8}Pu_{0.2}C$ (100 percent density) has been found to be representable by the equation

$$k = 0.0286 + 22.4 \times 10^{-6}\ t$$

where k is in cal/°C-sec-cm and t is in °C over the temperature range 250-660°C.

A 3M Model TC-200 thermal conductivity apparatus capable of measurements up to 1200°C is now being calibrated with vendor certified standards.

REFERENCES

1. W. C. Pritchard and R. L. Nance, "Studies on the Formation of Pu_2O_3 in the Sintering of PuO_2" Report LA-3493 (1966).
2. "Quarterly Status Report on Solid Plutonium Fuels Program for Period October 1 through December 31, 1963" LAMS-3054 (1964).
3. J. A. Leary, et. al. "Refractory Plutonium Fuel Materials" Third International Plutonium Conference, London (1965).
4. G. N. Rupert, Rev. Sci. Instr. 36 1629 (1965).
5. R. N. R. Mulford, F. H. Ellinger, G. S. Hendrix, and E. D. Albrecht, "The Plutonium-Carbon System" Plutonium 1960 p. 301, Cleaver-Hume Press, Ltd (1961).
6. Edmund K. Storms "A Critical Review of Refractories" LA-2942 (1964).
7. G. M. Campbell and J. A. Leary "Thermodynamic Properties of Pu Compounds from EMF Measurements I. Pu versus Ag in LiCl-KCl Eutectic" LA-3399 (1966).
8. G. M. Campbell and J. A. Leary, "Thermodynamic Properties of Plutonium Mononitride from Electromotive Force Measurements", J. Phys. Chem. 70, 2703 (1966).
9. M. B. Panish, F. F. Blackenship, W. R. Grimes and R. F. Newton, J´ Phy Chem 62, 1325 (1958).
10. J. C. Southard, J.A.C. 63, 3142 (1951).
11. R. Hultgren, R. L. Orr, P. D. Anderson and K. K. Delley, "Selected Values of Thermodynamics Properties of Metals and Alloys, John Wiley and Sons, Inc. New York, 1963.
12. V. A. Kirilin, A. E. Sheindlin and V. Ya. Chekevskoi, Doklady Akademii Nauk SSSR, 142, 1323 (1962).
13. J. A. Leary, R. L. Thomas, A. E. Ogard, and G. C. Wonn, "Thermal Conductivity and Electrical Resistivity of UC, (U, Pu)C, and PuC" Carbides in Nuclear Energy I 365 L. E. Russell et. al. MacMillan and Co. Ltd (1964)

PROJECT 808

COMPATIBILITY OF SODIUM BONDED (U,Pu)C AND (U,Pu)N FUELS WITH CLADDING MATERIALS

Person in Charge: D. B. Hall

Principal Investigators: R. H. Perkins
J. Leary

I. INTRODUCTION

The objectives of this program are to study the interactions of (U,Pu)C and (U,Pu)N with potential cladding materials and to develop the technology required for a sodium-bonded fuel element in which the fuel and cladding are compatible. The cladding materials to be studied include precipitation-hardening high temperature alloys, niobium, vanadium, and molybdenum alloys.

The compatibility of the carbide fuel with potential cladding materials will be determined as a function of the M/C ratio of the fuel. Hypo- and hyperstoichiometric mixed carbides, as well as fuel with stoichiometric composition, will be investigated. Carbides containing known and controlled small amounts of oxygen will be tested to determine the effect of oxygen on the sodium bond and on fuel-clad compatibility. Only stoichiometric (U,Pu)N fuels will be studied. The Pu/U ratio in all fuels will be maintained at 0.2.

The precipitation hardening stainless steels are promising cladding materials, since 17-4 PH stainless steel did not exhibit high temperature embrittlement during irradiation in LAMPRE to 2-3 x 10^{21} nvt. Initial studies will be concentrated on these alloys. The refractory metals and alloys with low fast neutron cross sections may also be technically satisfactory as cladding materials, though they are somewhat more expensive. Some effort will be expended on these materials. The utilization of

barriers to prevent the carburization of claddings due to carbon transport by sodium will be investigated.

All materials going into and coming out of test will be carefully characterized, using chemical analyses, nondestructive testing, physical properties measurements, and metallography. Fuels of known composition will be produced using methods developed by the Ceramic Plutonium Fuel Materials program (Project 807) at LASL. Sodium for bonding will be obtained from a hot trapped loop equipped with vacuum distillation apparatus for the determination of oxygen levels.

II. COMPATIBILITY TESTING

(J. Leary, F. B. Litton, B. J. Thamer, J. H. Bender, D. N. Dunning)

A. Carbide Fuels

1. Cladding Materials (F. B. Litton)

The objectives of this phase of the program are to study the interactions between (U,Pu)C and potential cladding materials and to develop the technology required for a sodium-bonded fuel element in which the fuel and cladding are compatible. The cladding materials that will be studied are high strength iron and nickel base, precipitation-hardening, and refractory metal alloys. The following is a tentative list of the clad materials that will be investigated:

(a) 316 stainless steel - austenitic stainless steel

(b) A-286 austenitic precipitation-hardening stainless steel

(c) AFC-77 and/or Alamar 362 - Martensitic precipitation-hardening stainless steel

(d) X-750 - nickel-based precipitation-hardening

(e) Incoloy 800 - low nickel alloy

(f) Hastelloy X (or X-280) - intermediate nickel alloy

(g) Inconel 625 - high nickel alloy.

(h) WF-11 - cobalt alloy

(i) Mo-½% Ti - molybdenum alloy

(j) Nb-1% Zr - niobium alloy.

Four hot trapped isothermal sodium loops are available for compatibility testing of ceramic fuels. Each of these loops will accommodate 16 test capsules. Each loop is being equipped with a distillation sampler for oxygen determination.

The initial screening tests will be carried out at 750°C for 2000 h. The most promising fuel-bond-clad combinations will then be tested in isothermal loops at several different temperatures for longer periods of time.

Later tests will include determining the effects of temperature gradients on fuels and cladding materials. Specific items to be investigated include the fundamentals of the mechanism of mass transport of fuel components under a temperature gradient, mass transfer under various temperature gradients over different lengths of fuel elements, the effects of gap width between fuel and cladding, the effect of oxygen content of the sodium bond, and a study of vented fuel capsules in which the fuel is exposed to the coolant sodium.

2. Synthesis and Fabrication of (U,Pu)C (M. W. Shupe, J. A. Leary)

One lot of $U_{0.80}Pu_{0.20}C$ was prepared by direct arc melting of the elements, followed by solution treatment for homogenization. The resulting ingot was crushed and ground to -325 mesh. A portion was also ball milled overnight. Pellets 0.40 in. diam x 0.3 in. tall were pressed at 60 tsi and sintered for 4 h in dry argon. Densification results shown in Table I indicate that sound pellets of good density can be produced.

Five additional lots of $U_{0.80}Pu_{0.20}$ C have been prepared by arc melting to determine the reproducibility of composition. All lots were prepared under identical conditions of arc current, arc time, number of melts, etc. Three lots were melted by means of a thoriated tungsten electrode, and two with a graphite electrode. After solution treatment, each lot was ground to -325 mesh for

Table I

Average Densification of $U_{0.80}Pu_{0.20}$ C Pellets

Milling Time, h	Pellet Density, g/cc (% Theoretical) unfired	sinitered
0	9.90(72.8)	11.0(81.0)
16	9.27(68.2)	12.7(93.1)
16	8.87(65.2)	12.6(92.4)

Note: Size range of powders after 16 h milling:
83% $\leq$ 2μ, 98% $\leq$ 5μ by count.

evaluation. One lot was purposely overloaded with carbon to form "hyperstoichiometric" carbide (MC + M_2C_3). This lot was then treated with pure hydrogen at 850°C. The carbon-to-metal atom ratio in this powder was reduced from 1.2 to 1.00 ± 0.01. Complete evaluation of the five lots, including chemical analyses, X-ray powder diffraction, pressing and sintering, and microstructure, is being continued.

B. Nitride Fuels (B. J. Thamer)

Among the advantages of the stoichiometric mononitride fuel are a higher density than the carbide or oxide, an easier preparation of the stoichiometric material, and a high thermodynamic stability with respect to feasible containers. The stability of a nitride fuel/sodium/clad combination is to be studied experimentally.

The nitride is to be solid solution of (depleted) UN and PuN with a Pu/U ratio of 0.2, except in about one-fourth of the cases when the nitride will be pure (depleted) UN. The test results with pure UN should help to differentiate between the behavior of PuN and UN, and also show the probable behavior for a fuel of ^{235}UN or ^{233}UN or a blanket of depleted UN. The nitride pellets should have:

1. The mononitride microstructure as shown by metallography and determinations of metal and sesquinitride phases by point count

2. An analyzed nitrogen content
3. A carbon content of 500 ppm maximum
4. An oxygen content of 500 ppm maximum
5. A spectrographic analysis
6. Total impurities of less than 2000 ppm.

The cladding materials that will be investigated include the following:

1. All materials that will be tested with (U,Pu)C fuels.
2. Armco iron
3. V-15% Ti-7.5% Cr.

The testing procedure will be identical to that outlined for (U,Pu)C fuels.

C. Post-test Examination (J. H. Bender, B. J. Thamer)

After an exposure of the fuel/sodium/clad at a given time and temperature, the clad will be cut open and the bulk of the sodium will be removed by melting and decantation. This operation will probably introduce some oxide into the residual sodium due to contaminants in the inert atmosphere of the drybox. It is planned to remove this oxide and the residual sodium with normal butyl alcohol. Tests indicate that a drop (0.2 g) of sodium dissolves in ½ - 1-½ h at room temperature depending on whether the oxide thickness is 0 or about 1 mm. In one experiment sodium was placed on a piece of cast UC containing 4.83 w/o C that had previously been metallographically mounted and examined. The sodium was removed with butyl alcohol and the UC was again examined metallographically. The UC was unchanged. Butyl alcohol has an advantage over ethyl alcohol in being relatively nonflammable. Representative carbide and nitride pellets have been requested for additional tests.

Specimens of (U,Pu)C are being employed in the development of metallographic techniques for the examination of this material. One sample which was stored overnight in a face-down position on an oil-soaked surface was destroyed, apparently by reaction with moisture in the air. It

was found that samples could be stored for several days in a desiccator that had been back-filled with helium. An alternate technique that appears to be satisfactory for overnight storage of (U,Pu)C specimens is immersion in Dow-Corning 200 silicone oil.

The normal procedure for the loading, testing and examination of capsules is as follows. One cubic centimeter of sodium and three weighed fuel pellets will be placed in each container in an inert atmosphere. The container will be welded closed in the presence of helium to facilitate leak checking. The container then will be exposed in a sodium loop with the loading end up.

After the exposure, the sodium will probably be removed by melting and decantation followed by the removal of residual sodium. The bulk sodium will be analyzed. The pellets will be reweighed if they are intact after removal. The extent of any attack or the presence of reaction layers will be determined during metallography. Microprobe analyses may be employed to obtain values of composition for affected base material, intergranular precipitates and reaction layers. X-ray diffraction analyses and hardness measurements may be made. In addition, the mechanical properties of the test container will be measured.

D. Planned Irradiations (EBR-II) (J. O. Barner)

The purpose of these irradiations is to evaluate candidate fuel pin systems for the fast power reactor program. The reference design selected by Los Alamos as the most promising system is a (1) sodium bonded, (2) single-phase (U,Pu)C fueled, (3) precipitation-hardened (or other high temperature alloy) alloy clad, fuel pin system.

The following general design criteria were determined for the first of the planned irradiations in EBR-II:

1. The fuel concept shall be a metal clad, unvented, sodium bonded, single phase (U,Pu)C fuel.
2. The nominal pin size shall be 0.3000 in. o.d. by 0.2800 in. i.d.
3. The fuel loading shall be 20% commercially available plutonium with the fuel enrichment adjusted to balance the heating rate in EBR-II.

4. The lineal power rating shall be 30 kW/ft (maximum),(i.e., approximately 26 kW/ft average).
5. The smear density for 6 of the 7 tests shall be 80% (75% for the seventh). The pellet density shall be 90% of theoretical for the 80% smear density tests and 85% of theoretical for the 75% smear density case.
6. The o.d. capsule wall temperature shall be 1300°F (centerline temperature approximately 2200°F).
7. Burnup will be varied at 1/2, 3/4, and 1 g fission/cm^3.
8. The cladding materials will be (1) 316 stainless steel, and (2) a material to be chosen soon based on availability in tubing form (a precipitation-hardened alloy would be most desirable).
9. The gas plenum size will be calculated to produce a reasonable hoop stress in the capsule wall (i.e., approximately 5000-8000 psi for low strength materials and 10,000-15,000 psi for high strength materials).

The following preliminary specifications are outlined below subject to revision as required at a later date:

1. Fuel Pellets
   (a) 0.265 ± 0.002 in. diam x 0.300 ± 0.005 in.
   (b) Single phase (U,Pu)C as shown by metallography at 100X, 200X, and 500X
   (c) Surfaces of the pellets are to be in the as-fired condition
   (d) During post-firing handling the pellets are to be kept as clean as possible
   (e) Immediately prior to storage in helium filled gas-tight containers the pellets are to be washed in absolute alcohol (or other suitable solvent) in an ultrasonic cleaner and vacuum dried
   (f) 20% ± 1% Pu (approximately 95% ^{239}Pu), 80% uranium (enrichment is unspecified at this time; it will be high)
   (g) Impurity levels, 200 ppm oxygen maximum, total all other impurities < 1500 ppm
   (h) Density 85% and 90% of theoretical density.

2. The Clad

(a) 0.300 ± 0.0015 in. x 0.2800 ± 0.0015 in., wall = 0.0100 ± 0.0015, ± 0.004 in./ft straightness

(b) Surface finish i.d. and o.d. = 32 μ in. (rms), maximum

(c) Heat treated as required.

3. The Sodium Bond

(a) Oxygen < 10 ppm

(b) Total all other impurities < 25 ppm.

4. The first test combinations are:

Test No.	Smear Density (%)	Pellet Density (%)	Clad (Stainless Steel)	g fission/cm^3
1	80	90	316	1/2
2	80	90	316	3/4
3	80	90	316	1
4	80	90	*	1/2
5	80	90	*	3/4
6	80	90	*	1
7	75	85	316	3/4

*Material not chosen at this time.

5. Follow-on tests will vary the cladding material as much as possible.

Calculations for the capsule design and information necessary for the proposal letter to ANL are underway. It is expected that the proposal for "Approval in Principle" for the first seven capsules to be inserted in EBR-II will be sent to ANL during the next quarter. The tentative schedule for insertion (depending on cladding availability and sodium bonding technique) calls for the capsules to be ready about March 1, 1967.

E. Loading Facility (D. N. Dunning)

A complete system for loading ceramic fuel and sodium into capsules of proposed cladding materials is being designed, fabricated and assem-

bled. The scheduled completion date for this facility is January 1, 1967. The components of this system, and their present status, are as follows:

1. Fuel Loading Station

   The glovebox that will be used for this purpose cannot be evacuated, so an inert atmosphere will be obtained by purging. The necessary modifications to the glovebox have been completed, and gas lines and fuel loading equipment are being installed.

2. Sodium Purification Loop

   This box can be evacuated prior to the introduction of helium. It is capable of maintaining a high quality helium environment. Extrusion equipment will be used to provide known amounts of sodium for bonding. The extrusion and loading equipment are in the design stage. The vacuum piping and equipment for this box are being assembled.

4. Welding Box

   This final closure and sodium bond station consists of an inert gas glovebox, welding equipment and fixtures and a vibratory furnace. The welding fixture and equipment for making closure welds on capsules are on hand and ready for assembly. The vibratory furnace, which will be used to obtain a good sodium bond between fuel and clad, is in the design stage.

PROJECT 811

REACTOR NUCLEAR ANALYSIS METHODS AND CONCEPT EVALUATIONS

Person in Charge: D. B. Hall

Principal Investigator: G. H. Best

I. APPLICATION OF CONTINUOUS ANALYTIC CONTINUATION TO REACTOR KINETIC PROBLEMS

(J. C. Vigil, B. M. Carmichael)

Continuous analytic continuation is a method of solving reduced or point reactor kinetics equations by expanding those variables that are analytic functions of time in Taylor series over successive intervals in the time domain. Its properties have been investigated theoretically and verified by comparison with analytic solutions in cases for which analytic solutions are available.

Continuous analytic continuation yields a definitive criterion for the magnitude of the time step in each point in a transient. This criterion allows the time step to expand or contract, according to the behavior of the neutron level within each interval. The use of this criterion to determine the time step guarantees that the error in the results increases at most linearly with the number of time steps. That is, the fractional error after n time steps is bounded by $n\varepsilon$, where ε is the error criterion ($\varepsilon << 1$). The error criterion determines the maximum truncation error in each Taylor expansion.

This method is well suited to digital computer application. A computer program based on continuous analytic continuation, ANCON, has been written for the IBM 7094 computer.[1] The program is written in modular form:

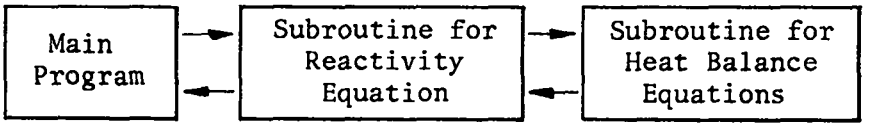

The equation for the reactivity and the associated heat balance equations are introduced by the use of subroutines, so that any type of reactivity variation (including feedback) can be represented by simply replacing the proper subroutine. ANCON has been found to be as much as 25 times as fast as the RTS code[2] for excursions in fast reactors.

The ANCON code has been used for kinetics calculations for the UHTREX Safety Analysis (LA-3356). Six delayed neutron groups were used, and the detailed variation of the impressed reactivity with time due to rod motion and rod position was taken into account in all calculations. Three types of transient were considered:

1. Rod withdrawal accidents starting at essentially zero initial power,
2. Rod withdrawal accident starting at 3 MW delayed critical,
3. Scrams from 3 MW delayed critical.

ANCON has also been used to solve the problem defined by:

$$\frac{dN(t)}{dt} = \frac{1}{\Lambda}[\rho(t) - \beta]\, N(t) + \lambda C(t) \qquad (1)$$

$$\frac{dC(t)}{dt} = \frac{\beta}{\Lambda} N(t) - \lambda C(t) \qquad (2)$$

$$\rho(t) = \rho_o \sin(\pi t/T) \qquad (3)$$

If ρ_o and T are related by the expression

$$\rho_o = \frac{8\beta}{8 + \lambda T}$$

and if

$$\rho_o < \beta,$$

equations (1) through (3) give a crude simulation of a slow self-limiting transient.

For problems in which $\rho(t)$ is less than β throughout the transient, particularly with small Λ, a straightforward application of the basic method described in LA-3518 is very inefficient. However, the basic method has been modified for such cases so that the time step is determined by the delayed neutron precursors, thus yielding time steps two or more orders of magnitude larger than the basic method with little, if any, sacrifice in accuracy.

Numerical solutions to equations (1) through (3) using the modified method are shown in Fig. 1 for a full cycle ($0 \leq t \leq 2T$) and for several values of ρ_o and T. Other constants used were:

$\Lambda = 10^{-8}$ sec

$\beta = 0.0079$

$\lambda = 0.007$ sec^{-1}

$N(0) = 1$

$C(0)$ = equilibrium value.

The peak value of N(t) and the value of t at the peak for the cases shown in Fig. 1 are compared in Table I with the analytic ($\Lambda = 0$ approximation) results. (For $\Lambda = 10^{-8}$ sec, the error in the analytic approximation is negligible.) The numerical results using analytic continuation agree, within the accuracy predicted by the method, with the exact solutions.

TABLE I

COMPARISON OF ANALYTIC AND NUMERICAL RESULTS

T (sec)	ρ_o	Peak N(t)		Time at peak (sec)	
		Analytic Continuation	Analytic Solution	Analytic Continuation	Analytic Solution
50	5.33333×10^{-3}	61.37	61.53	39.1	39.1
150	3.23274×10^{-3}	95.56	95.82	137.3	137.3
250	2.31927×10^{-3}	113.2	113.5	237.2	237.1
350	1.80830×10^{-3}	123.6	123.8	337.1	337.1

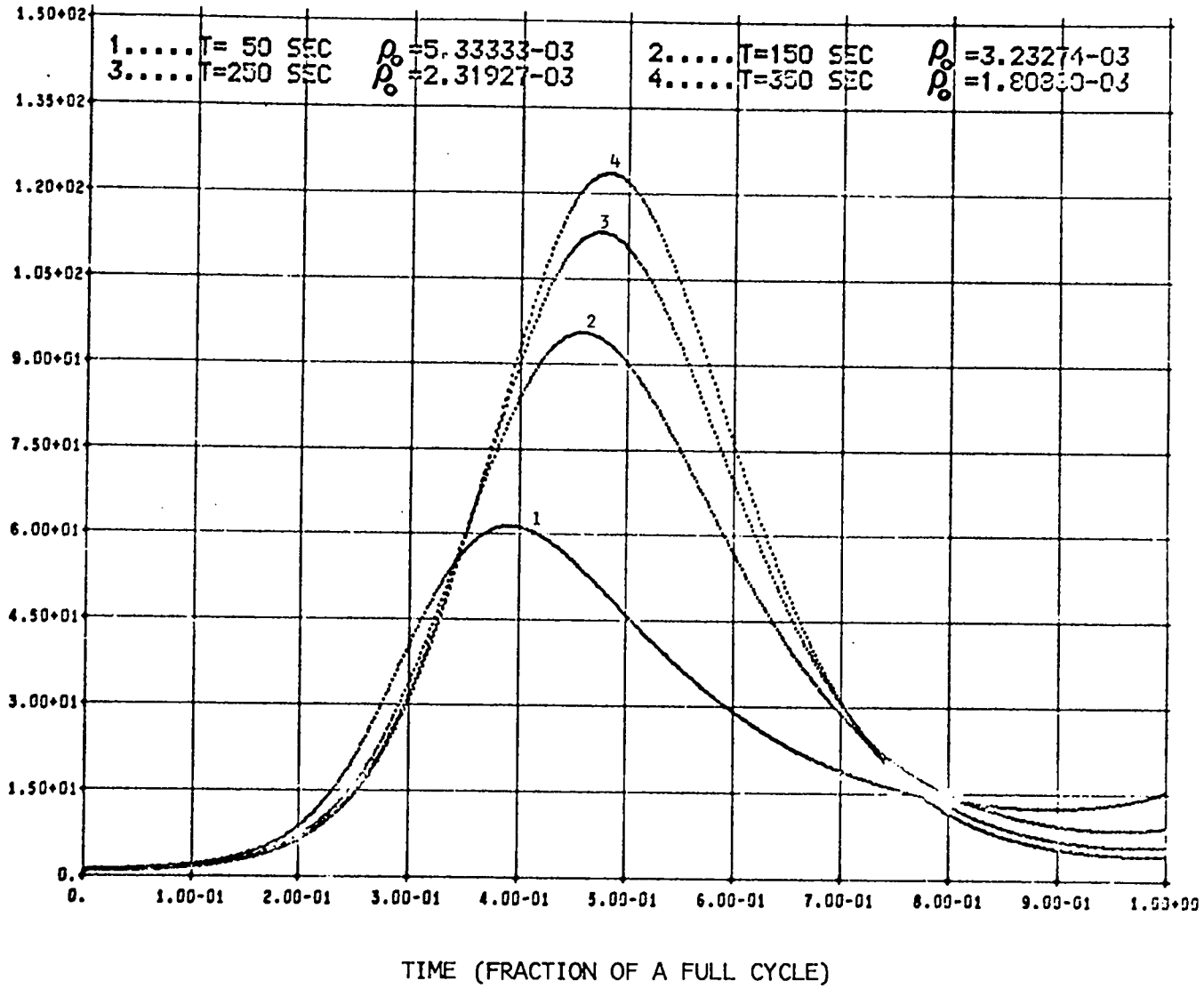

Fig. 1. Numerical Solutions of Eqs. 1 through 3 for Various Values of T and ρ_0.

II. PREPARATION AND MAINTENANCE OF REACTOR CODE PACKAGES

(J. J. Prabulos, W. H. Hannum)

An iterative transport theory burnup program, DTFBUR, to be used in survey life-history studies of various plutonium-fueled fast reactor systems, has been substantially completed. For each of a specified number of time intervals, the code computes the neutron flux distribution as a discrete ordinates solution of the Boltzmann transport equation. This calculated flux distribution is then used to determine the change in isotopic composition during the time width. Isotopes permitted include ^{235}U, ^{236}U, ^{238}U, ^{239}Np, ^{239}Pu, ^{240}Pu, ^{241}Pu, ^{242}Pu, and "fish-pium," (FP) a pseudo fission product pair. The burnup differential equations may be solved either regionwise or pointwise at the option of the user.

The DTFBUR package consists of fifteen subroutines, and is called by a simple program which permits successive problems to be executed, even if errors occur in individual problems. Thirteen of the subroutines are modified versions of subroutines found in the DTF-IV code.[3] The basic function of these subroutines is to direct the calculational flow and perform the multigroup flux calculation at the beginning of each time step. The other two subroutines are BURN, which solves the burnup differential equations regionwise, and POBURN, which solves the isotopic equations pointwise. Both burnup subroutines are based on the solution method of the SIZZLE reactor burnup program.[4]

The basic features of DTFBUR are:

1. A different type of flux calculation (k/alpha/concentration/delta/radius) may be performed at the beginning of each time step. This permits the simulation of a reactor in which different methods of control are used during the lifetime (e.g., control rod movement part of the time and reflector control at other times).

2. The concentration search subroutine has been modified to search directly on densities, rather than cross-section mixtures, so that isotopic changes during a search are taken into account in subsequent burnup calculations. Final densities resulting from a concentration search are printed out at the end of each flux calculation.
3. The number of time intervals for burnup and the length of each interval are specified by the user. This feature permits variable time step widths during a calculation.
4. Burnup calculations are performed only in those regions specified in the input data.
5. Region-dependent microscopic cross sections for each burnup element may be used in the burnup equations, if desired.
6. The point burnup subroutine contains a section which integrates calculated point burnup densities to obtain regional averages. These regional averages are used in the calculation of the macroscopic cross sections at the beginning of the succeeding time step. If these average densities are then changed in a concentration search, new point densities for the search elements are computed from the point values in core storage and the ratios by which the average densities were changed in the concentration search.
7. Atom densities and masses are printed out for the burnup elements at the end of each time interval.
8. The program contains a restart dump option for point densities and fluxes.

A 15-group cross-section set was prepared for the burnup analyses. It is based on the 18-group set of C. B. Mills,[5] with the last four groups replaced by a single thermal group. Sources of data for the cross sections are listed in Table II. Since no cross sections with the Mills group structure are available for the elements cobalt and cerium, which are present in liquid plutonium reactors, cross-section sets for

TABLE II

CROSS-SECTION DATA FOR LIFE-HISTORY ANALYSES

Isotope	Source of Data Groups 1-14	Source of Data Group 15
Ta	Mills	Lethargy-weighted average of Mills[5] groups 15-18
^{238}U	Mills	Library 9W088[6]
^{239}Np	Library 9W088	Library 9W088
^{239}Pu	Mills	Library 9W088
^{240}Pu	Mills	Library 9W088
^{241}Pu	Library 9W088	Library 9W088
^{242}Pu	Library 9W088	Library 9W088
FP (fishpium)	Library 9W088	Library 9W088
Fe	Mills	Library 9W088
Cr	APDA Memo P-62-336	Tempest-Maxwellian Distribution for T = 950°F
Ni	APDA Memo P-62-336	Tempest-Maxwellian Distribution for T = 950°F
Na	Mills	Library 9W088
C	Mills	Library 9W088
O	Mills	Library 9W088
^{235}U	Mills	Library 9W088
^{236}U	Library 9W088	Library 9W088
Mo	Mills	Lethargy-weighted average of Mills groups 15-18
Nb	Mills	Lethargy-weighted average of Mills groups 15-18

these elements are being compiled. Values for the first six groups will be taken from the Hansen-Roach[6] set, whose energy structure is identical with that of the Mills set above 17 keV. Transport values for groups 7-15 will be determined by the integration of point values in BNL-325,

and absorption values will be calculated by lethargy-weighting of values in the Hansen-Roach set. Scattering cross sections will then be calculated from the transport and absorption cross sections.

We are planning to compare iterative diffusion-burnup and transport-burnup calculations for various fast reactor systems. The SIZZLE diffusion-burnup program was obtained from the Argonne Code Center for this work. In order to permit the execution of the original chain-type program on the IBM 7030 computer, the main programs in each chain were designated as subroutines, and the program was rewritten to accept cross sections in DTF format. In addition, SIZZLE was modified to perform burnup calculations with up to 18 neutron energy groups and with variable time-step widths.

III. ADVANCED SYSTEM TECHNICAL EVALUATIONS

(J. J. Prabulos, W. H. Hannum)

The world standard of comparison for fast breeder reactors is the sodium-cooled, oxide-fueled, stainless-clad system.[7] Many other systems have been proposed, including variations in fuels, coolants, clads, temperatures, geometries, physical form of various components, fuel cycles, coolant cycles, plant features, and other properties. Extensive technical evaluation of these proposals is necessary to determine their value. The basis for these evaluations should be the performance characteristics of the various sodium-cooled, oxide-fueled, stainless-clad large-scale system studies.

A life-history analysis of the 1000 MWe Westinghouse modular fast breeder reactor has been carried out using the DTFBUR transport burnup program (see Section II). Calculations were carried out for an average core burnup of 100,000 MWD/MT of heavy atom. Six burnup time intervals were employed having the following widths in days:

(1)	50.0	(4)	200.0
(2)	50.0	(5)	300.0
(3)	100.0	(6)	397.6

Isotopic masses in the carbide-fueled core as a function of time are given in Table III, results for the oxide blanket are given in Table IV, and some selected design parameters are listed in Table V.

TABLE III

WESTINGHOUSE MODULAR FAST BREEDER REACTOR

CORE MASSES (kg) AS A FUNCTION OF TIME

Time (days)	^{238}U	^{239}Np	^{239}Pu	^{240}Pu	^{241}Pu	^{242}Pu	FP*
A. Vacuum Boundary Condition (Outer Edge)							
0	3024	0.0	589.6	260.5	36.6	9.0	0.0
50	3012	0.62	583.5	260.3	36.6	9.0	16.9
100	3001	0.63	578.1	260.1	36.2	8.9	33.9
200	2977	0.63	567.7	259.6	35.6	8.9	67.4
400	2930	0.64	548.2	258.7	34.4	8.7	133.5
700	2858	0.65	522.4	257.2	32.8	8.5	230.2
1097.6	2760	0.66	494.0	255.3	31.1	8.2	354.0
B. Reflective Boundary Condition (Outer Edge)							
50	3012	0.62	583.5	260.3	36.6	9.0	16.9
100	3001	0.62	578.1	260.1	36.2	8.9	33.6
200	2978	0.62	567.7	259.6	35.6	8.9	66.8
400	2931	0.62	548.4	258.6	34.4	8.7	131.6
700	2862	0.62	523.0	257.1	32.9	8.5	225.3
1097.6	2771	0.62	495.1	255.0	31.3	8.2	342.5

*Fission product pairs.

TABLE IV

WESTINGHOUSE MODULAR FAST BREEDER REACTOR

BLANKET MASSES (kg) AS A FUNCTION OF TIME

Time (days)	^{235}U	^{236}U	^{238}U	^{239}Np	^{239}Pu	^{240}Pu	^{241}Pu	^{242}Pu	FP*
A. Vacuum Boundary Condition (Outer Edge)									
0	21.2	0.0	7171	0.0	0.0	0.0	0.0	0.0	0.0
50	21.1	0.03	7161	0.57	7.9	0.0081	3.84×10^{-6}	1.32×10^{-9}	0.7
100	20.9	0.06	7153	0.58	16.4	0.0298	2.75×10^{-5}	1.87×10^{-8}	1.5
200	20.6	0.13	7134	0.58	33.6	0.1142	2.07×10^{-4}	2.79×10^{-7}	3.2
400	19.9	0.25	7096	0.60	67.8	0.4525	1.63×10^{-3}	4.43×10^{-6}	7.5
700	18.9	0.44	7036	0.62	119.0	1.4092	8.94×10^{-3}	4.33×10^{-5}	16.0
1097.6	17.5	0.66	6952	0.65	186.0	3.5682	3.58×10^{-2}	2.79×10^{-4}	31.4
B. Reflective Boundary Condition (Outer Edge)									
50	21.0	0.04	7158	0.82	11.3	0.034	6.752×10^{-5}	6.26×10^{-8}	0.8
100	20.8	0.09	7145	0.84	23.6	0.115	4.492×10^{-4}	7.63×10^{-7}	1.8
200	20.3	0.18	7118	0.85	48.0	0.398	2.919×10^{-3}	9.23×10^{-6}	4.1
400	1-.4	0.36	7063	0.87	96.6	1.383	1.861×10^{-2}	1.10×10^{-4}	10.1
700	18.1	0.60	6976	0.91	169.0	3.833	8.149×10^{-2}	8.57×10^{-4}	27.8
1097.6	16.4	0.88	6854	0.96	263.0	8.935	2.663×10^{-1}	4.16×10^{-3}	46.7

*Fission product pairs.

TABLE V

WESTINGHOUSE MODULAR FAST BREEDER REACTOR

SELECTED DESIGN PARAMETERS AS A FUNCTION OF TIME

Time (days)	Breeding Ratio	Core Power Fraction	Core Peak Average Power	Blanket Peak Average Power	Fraction Neutrons Control	Fraction Neutrons Fission Product
A. Vacuum Boundary Condition (Outer Edge)						
0	1.146	0.9616	1.554	3.012	0.1521	0.0
50	1.159	0.9582	1.547	2.933	0.1445	0.0012
100	1.171	0.9544	1.540	2.856	0.1370	0.0026
200	1.194	0.9467	1.525	2.730	0.1221	0.0053
400	1.232	0.9308	1.500	2.549	0.0952	0.0110
700	1.280	0.9047	1.462	2.369	0.0563	0.0201
1097.6	1.317	0.8685	1.422	2.216	0.0143	0.0329
B. Reflective Boundary Condition (Outer Edge)						
0	1.372	0.9571	1.545	2.709	0.1561	0.0
50	1.387	0.9496	1.536	2.484	0.1488	0.0013
100	1.400	0.9424	1.528	2.342	0.1422	0.0026
200	1.423	0.9287	1.512	2.165	0.1299	0.0052
400	1.463	0.9004	1.481	1.956	0.1065	0.0107
700	1.502	0.8547	1.438	1.767	0.0776	0.0190

REFERENCES

1. J. C. Vigil, "Solution of the Nonlinear Reactor Kinetics Equations by Continuous Analytic Continuation," LA-3518, in press.
2. G. R. Keepin and C. W. Cox, Nucl. Sci. Eng. 8, 670 (1960).
3. K. D. Lathrop, "DTF-IV, a FORTRAN-IV Program for Solving the Multigroup Transport Equation with Anisotropic Scattering," LA-3373 (1965).
4. D. P. Satkus and H. P. Flatt, "SIZZLE, A Fast or Intermediate Reactor Burnup Code," NAA Program Description, AI-64-MEMO-183 (1964).
5. "Los Alamos Group-Averaged Cross Sections," L. D. Connolly, ed., LAMS-2941 (1963).
6. "Feasibility Study of a 1000-MWe Sodium-Cooled Fast Reactor," Atomics International, NAA-SR-11378 (1965).
7. R. V. Moore and S. G. Fawcett, "Present and Future Types of Fast Breeder Reactors," BNES Conf. on Fast Breeder Reactors, Paper 117 (May 1960).

PROJECT 812

TESTING AND EVALUATION OF NEUTRON CROSS SECTIONS FOR REACTOR CALCULATIONS

Person in Charge: D. B. Hall

Principal Investigator: G. H. Best

I. EVALUATION OF NUCLEAR DATA

(R. J. LaBauve, M. E. Battat, D. J. Dudziak)

For the evaluation of various fast breeder reactor concepts, good analytical techniques and cross sections are necessary. Valid comparisons between different concepts depend on minimization of differences in results due to the methods of analysis. To this end, The Los Alamos Scientific Laboratory is cooperating with other AEC laboratories in the development of a uniform set of evaluated nuclear cross-section data and associated processing codes. LASL is preparing the data for ^{6}Li and ^{7}Li to be incorporated in the initial version of the nuclear data file (ENDF/B.)

Data for these isotopes from the nuclear data file currently in use at LASL (the Mu code, the AWRE nuclear data file,[1] and from H. Alter of Atomics International have been considered for inclusion in ENDF/B. The Atomics International data is the most complete, and will therefore be incorporated in ENDF/B. The data include elastic scattering angular distributions in the form of the Legendre coefficients, and values of $\bar{\mu}_{LAB}$, ζ, and γ.

II. TESTING OF MULTIGROUP CROSS-SECTION SETS

(M. E. Battat, D. J. Dudziak, R. J. LaBauve)

Before a multigroup cross-section set is used in reactor calculations, theory must be compared with experiment. In general, comparisons of calculated critical masses with the results of criticality experiments are

difficult to interpret for two reasons. First is the possibility of compensating errors when cross sections for several elements are needed to calculate the system. The second is the uncertainty introduced by and the additional calculations required to account for heterogeneity effects. By comparing calculated central reactivity worths with experimental values, one can examine a single element at a time and thus simplify the evaluation.

A comparison of the Hansen-Roach[2] and Russian[3] cross-section sets has been continued. Central reactivity worths in Jezebel have been computed for Fe, Ta, Na, ^{238}U, ^{235}U, and Ni. Using shielded cross sections for the U isotopes, central reactivity contributions in ZPR-VI (Assembly 2) have been obtained for ^{235}U, depleted U, Fe, B and Ni.

We were invited to participate in a world-wide comparison of calculated parameters for ZPR-3 Assembly 48. This is a plutonium-fueled, soft-spectrum, simple-geometry critical assembly which is being studied at ANL. Our participation has been mainly in the calculation of central reactivity worths of about a dozen elements. The calculations were done in spherical geometry [DTF code[4]]; the Hansen-Roach and Russian cross-section sets were used. The results obtained agreed well with those obtained from perturbation theory calculations. Results of our calculations have been transmitted to W. G. Davey (ANL) for use in a paper on the intercomparison of calculations to be presented at the International Conference on Fast Critical Experiments and Their Analysis, at Argonne on October 10-13, 1966.

Central reactivity worths for "small" samples in ZPR-6, Assembly 2 and Jezebel were calculated using perturbation theory with both the Hansen-Roach and Russian cross-section sets. A paper describing these calculations has been written and will be presented at the International Conference at Argonne.

REFERENCES

1. Susan M. Miller and K. Parker, "List of Data Files Available in the UKAEA Nuclear Data Library as of 15 April 1965," AWRE 0-55/65.

2. "Los Alamos Group-Averaged Cross Sections," L. D. Connolly, ed., LAMS-2941 (1963).

3. "Group Constants for Nuclear Reactor Calculations," I. I. Bondarenko, ed., Consultants Bureau translation (1964).

4. K. D. Lathrop, "DTF-IV, a FORTRAN-IV Program for Solving the Multigroup Transport Equation with Anisotropic Scattering," LA-3373 (1965).

PROJECT 814

EVALUATION OF CONTINUOUS MASS SPECTROMETRIC ANALYSIS OF SODIUM SYSTEM COVER GAS

Person in Charge: D. B. Hall

Principal Investigators: G. H. Best

I. INTRODUCTION

Cover gas analyzers for high-temperature sodium-cooled reactors must be capable of detecting impurities such as nitrogen, oxygen, hydrogen, carbon dioxide, and methane in the cover gas with a sensitivity adequate to measure impurities from the part per million range to the per cent range. The analyses should be performed with an accuracy of at least 5% and a reproducibility of about 1%.

Gas chromatographs are commonly used as gas analyzers for reactors. These vary in accuracy from instrument to instrument, and from operator to operator. Mass spectrometers are significantly more accurate for gas analyses, but cannot be operated at the high temperatures necessary for the analysis of sodium cover gas. High temperature on-line operation is necessary for this type of analysis because of the tendency for sodium compounds to occur in the cover gas, providing a background in the analysis, and thus making an analysis in the part per million range difficult.

II. HIGH TEMPERATURE, RESIDUAL GAS ANALYZER

(N. G. Wilson, D. C. Kirkpatrick)

A wide range bakeable quadrupole mass filter residual gas analyzer, which has recently become available commercially, can be operated up to above 300°C. Work presently in progress with high temperature sampling systems indicates that the capability of the analyzer can probably be extended to temperatures of 500-600°C. Special feedthrough devices in

the analyzer assembly will allow on-line operation at that temperature. A field emission ion source will reduce fragmentation of molecules in the analyzer. A digital data handling system will allow real-time inspection of changes in the cover gas composition and on-line data reduction by a digital computer, which may be integrated into a general reactor monitoring and control system.

Initial investigation of the effects of the higher operating temperature for the analyzer has revealed three basic areas of concern:

1. sampler valve flow control,
2. quadrupole operation, and
3. demountable seals.

It appears that items 1 and 3 can be achieved fairly easily, but item 2 may present a problem because it appears that the present quadrupole can not be operated at temperatures much greater than 300°C. However, it is believed that this limitation can be overcome.

Hardware for testing a seal at 700°C has been ordered. This seal will utilize a pure nickel gasket in a commercial ultra-high vacuum flange fastened with special high-temperature bolts. This system should perform under prolonged high-temperature operation, as well as under thermal cycling. In addition to this type of seal, special high-temperature gaskets of nickel-plated Inconel X have been ordered to permit evaluation of two other types of seals.

A flow splitting sampling valve recently placed on the market has been ordered for evaluation as a sampler valve. The valve in its present configuration can not operate at required temperatures; however, suitable modification should not be difficult.

PROJECT 816

ADVANCED MEASUREMENT AND ANALYSIS TECHNOLOGY

Person in Charge: D. B. Hall

Principal Investigators: G. H. Best

I. CORRELATION OF NONDESTRUCTIVE TEST WITH LIQUID METAL COOLANT LEAKS

(N. G. Wilson, H. M. Ruess)

Helium mass spectrometer leak detection is customarily used as a quality control method during fabrication of sodium-containing reactor coolant systems. It is usually specified that such systems should show no leaks in excess of 10^{-7} to 10^{-8} standard cm^3/sec helium, although experience at LASL has shown that for loop temperature above 500°C, a nonrepairable helium leak greater than 10^{-9} standard cm^3/sec will probably result in a sodium leak within the first year of operation. By studying mechanisms and characteristics of helium molecular transport rates through microscopic penetrations in metals, we hope to correlate helium leak rates with those of liquid metal coolants.

This study will utilize fabricated stainless steel leaks with a range of helium leak rates. Each of these will be incorporated into a small sodium system which will be held at a predetermined temperature until sodium leakage occurs.

For fabrication of leaks, a special die has been developed to compress fully annealed, type 304 stainless steel tubing. To prepare the tubing for compression, five methods have been used:

1. Degreasing
2. Reaming and degreasing
3. Degreasing, reaming, and electropolishing
4. Degreasing and chempolishing
5. Electropolishing.

Metallography of the compressed tubes has shown that reaming and degreasing (process 2) is the most promising approach. In order to improve the control over leak-forming conditions, an apparatus similar to that used in some NASA friction studies is being assembled. This apparatus will allow ultrahigh vacuum bakeout of the tubes prior to compression and pressure control during compression in order to limit the amount of gas adsorbed on the tube walls.

Design of an appropriate static sodium system and furnace is continuing.

II. GAMMA SCANNING TECHNIQUES

(D. M. Holm, W. M. Sanders, B. M. Moore)

Some interesting information is potentially available from studies of fission product concentrations and distributions in irradiated fuel and blanket elements. As examples, the relative amount of gaseous isotopes present can be used as a measure of the integrity of the cladding, the short-lived isotopes can give a measure of the recent operating history, and the long-lived isotopes can give a measure of the total burnup. The usefulness of the gamma scanning technique is increased as scanning techniques are tried. Techniques which permit better gamma ray energy resolution, automated data acquisition, and selective suppression of computer phenomena in the detection system are being developed. These are directly applicable to studies of fission product distributions in sodium (Project 801).


RECEIVED
NOV 2 1966
Los Alamos
Scientific Laboratory
P. O. Box 1663
Mail & Records